

**ADDITIVE INCORPORATION IN THE POLYETHYLENE
ORIENTATION-CROSSLINKING PROCESS**

by

Ognian Kamenov

**A thesis submitted in conformity with the requirements
for the Degree of Master of Applied Science
Graduate Department of Chemical Engineering and Applied Chemistry
University of Toronto**

© Copyright by Ognian Kamenov, 1996



**National Library
of Canada**

**Acquisitions and
Bibliographic Services**

**395 Wellington Street
Ottawa ON K1A 0N4
Canada**

**Bibliothèque nationale
du Canada**

**Acquisitions et
services bibliographiques**

**395, rue Wellington
Ottawa ON K1A 0N4
Canada**

Your file Votre référence

Our file Notre référence

The author has granted a non-exclusive licence allowing the National Library of Canada to reproduce, loan, distribute or sell copies of this thesis in microform, paper or electronic formats.

The author retains ownership of the copyright in this thesis. Neither the thesis nor substantial extracts from it may be printed or otherwise reproduced without the author's permission.

L'auteur a accordé une licence non exclusive permettant à la Bibliothèque nationale du Canada de reproduire, prêter, distribuer ou vendre des copies de cette thèse sous la forme de microfiche/film, de reproduction sur papier ou sur format électronique.

L'auteur conserve la propriété du droit d'auteur qui protège cette thèse. Ni la thèse ni des extraits substantiels de celle-ci ne doivent être imprimés ou autrement reproduits sans son autorisation.

0-612-45451-7

Canada

ABSTRACT

The subject of this work is additive incorporation into polyethylene to further the development of a new polymer orientation-cross linking process. Two additives, a photo-initiator (benzophenone, BP) and a cross-linker (tri allyl cyanurate, TAC) are involved. The objectives were to devise a continuous method for incorporating the additives, to develop a Fourier Transform Infrared Spectrometer (FTIR) method of characterizing the additive concentration in the polymer and to investigate the effect of processing variables on additive concentration. Discovering the source of additive loss during processing was an important motivation for the work. All three objectives were accomplished. To incorporate the additives continuously (one of which was a liquid and the other a sticky solid) the phase diagram for their combination was elucidated. It was found that a 50:50 mixture was a stable liquid at room temperature that could be pumped into the process and provided the needed concentration level. An FTIR method was developed that permitted both average concentration of each additive and the concentration profile of additive across the diameter of the extruded strand to be determined. Finally, the additive incorporation method and the FTIR analytical technique were used together with processing runs to examine the effect of processing variables. Additive loss was found to be due to accumulation of the additives on the wall of the extruder. Evaporation of additive was found a distant secondary factor. Based on this result, higher additive concentrations that had ever previously been obtained (1.3 wt.% BP and 1.5 wt.% TAC) were accomplished by incorporating the additive in two stage processing. Experimental residence time distributions were obtained using BP and TAC mixed with silicone oil (a completely non-volatile additive) as tracer. These provided additional evidence that additive losses are not due to evaporation.

ACKNOWLEDGEMENT

I would like to thank Professor S. T. Balke for all his guidance, encouragement and patience during this work.

I wish to thank the Manufacturing Research Corporation of Ontario (MRCO) for financial support of this work.

I would like to express my appreciation to Mr. M. Tempel, Mr. A. Prins, Mr. A. Karami and all my friends for their help and assistance.

Finally, I would like to express my gratitude to my mother for all her love and support.

TABLE OF CONTENTS

	PAGE
ABSTRACT	ii
ACKNOWLEDGEMENTS	iii
TABLE OF CONTENTS	iv
LIST OF FIGURES	vi
LIST OF TABLES	viii
1.0 INTRODUCTION	1
2.0 THEORETICAL ASPECTS	2
2.1 Overview	2
2.2 Polymer Orientation-Crosslinking Process	2
2.2.1 Methods of Introducing BP and TAC	8
2.2.2 Dry Blending	9
2.2.3 Direct Feed	10
2.2.4 Basic Aspects of Additive Incorporation	11
2.3 Analysis of Additive Concentration	12
2.3.1 Principle of FTIR and FTIR Microscopy	13
2.3.2 Quantitative FTIR Analysis	18
2.4 The Effect of Processing Variable on Additive Concentration	20
3.0 EXPERIMENTAL	25
3.1 Materials	25
3.2 Equipment	26
3.2.1 Additive Incorporation by Extrusion	26
3.2.2 Additive Incorporation with a High-Intensity Mixer	27
3.3 Experimental Procedure	27
3.3.1 Preparation of a Liquid Mixture of Additives	27
3.3.2 Additive Incorporation by Extrusion	28
3.3.3 Additive Incorporation with High-Intensity Mixer	30

	PAGE
3.4 Analytical Methods	30
3.4.1 Quantitative FTIR Spectroscopy	30
3.5 Residence Time Distribution	32
4.0 RESULTS AND DISCUSSIONS	35
4.1 Development of a Continuous Method of Additive Incorporation	35
4.2 Additive Profiles	36
4.2.1 Radial Profile	36
4.2.2 Axial Profile	37
4.3 Effect of Processing Variables	40
4.3.1 Extrusion Conditions	40
4.3.2 Input Additive Concentration	41
4.4 Two Stage Incorporation	44
4.5 Extruder Residence Time Distribution	46
4.6 Additional Evaluation of Effect of Temperature	
by Use of Tree-Component Additive Mixture	51
4.7 Additive Incorporation with High Intensity Internal Mixer	53
5.0 CONCLUSIONS	55
6.0 NOMENCLATURE	56
7.0 REFERENCES	57
APPENDIX I Properties of Materials Used	61
APPENDIX II Jablonski Diagram	63
APPENDIX III MIR Spectrum of Polyethylene, BP, and TAC	65
APPENDIX IV Calibration Data	71
APPENDIX V Derivations of Equations and Sample Calculations	79
APPENDIX VI List of Selected Vibrational Modes	82
APPENDIX VII Analysis of Variance for 2³ Factorial Design	84

LIST OF FIGURES

		PAGE
Figure 2.1	Schematic of PCO Process	2
Figure 2.2	Reactions of Benzophenone to UV Radiation	4
Figure 2.3	Effect of Benzophenone on Crosslinking Rate	5
Figure 2.4	Effect of TAC on Crosslinking Rate	6
Figure 2.5	Reaction Scheme of Photo-cross-linking of Polyethylene	7
Figure 2.6	Effect of TAC on Homogeneity of UV-crosslinked PE	8
Figure 2.7	Phase Equilibrium Diagram of Two Component System	11
Figure 2.8	Entire Electromagnetic Spectrum	13
Figure 2.9	Schematic of Molecular Energy Levels	15
Figure 2.10	Vibrational Modes of C-H Bonds in Methylene Group	16
Figure 2.11	Schematic of Polymer Orientation-Crosslinking Process	20
Figure 2.12	Plot of Exit Age Distribution Function vs Normalized Time	24
Figure 3.1	Schematic of the Extrusion System	26
Figure 3.2	Schematic of the Location of Additive Insertion Port	27
Figure 3.3	Schematic of Sample Preparation Technique	31
Figure 4.1	Phase Equilibrium Diagram of BP-TAC Mixture	35
Figure 4.2	Concentration Profile of BP across PE-extrudate Cross Section	36
Figure 4.3	Concentration Profile of TAC across PE-extrudate cross section	36
Figure 4.4	Concentration Profile of BP along Extrudate length	37
Figure 4.5	Concentration Profile of TAC along Extrudate length	37
Figure 4.6	Concentration Profile of BP along Extrudate length	38
Figure 4.7	Concentration Profile of TAC along Extrudate length	38
Figure 4.8	Standard Deviation of BP Concentration as a Function of Extruder Conditions	39

	PAGE	
Figure 4.9	Standard Deviation of TAC Concentration as a Function of Extruder Conditions	39
Figure 4.10	Output Concentration of BP as a Function of Input Additive Concentration	42
Figure 4.11	Output Concentration of TAC as a Function of Input Additive Concentration	43
Figure 4.12	Loss of BP as a Function of Input Additive Concentration	43
Figure 4.13	Loss of TAC as a Function of Input Additive Concentration	44
Figure 4.14	% wt. BP Incorporated during the Two Stage Incorporation Process	45
Figure 4.15	% wt. TAC Incorporated during the Two Stage Incorporation Process	45
Figure 4.16	Tracer Concentration (BP) in Extrudate versus Time	46
Figure 4.17	Residence Time Distribution Function as a Function of Extruder Conditions	47
Figure 4.18	Mean Residence Time as a Function of Barrel Temperature	47
Figure 4.19	Tracer Concentration (TAC) in Extrudate versus Time	48
Figure 4.20	Residence Time Distribution Function as a Function of Extruder Conditions	48
Figure 4.21	Mean Residence Time as a Function of Barrel Temperature	49
Figure 4.22	Residence Time Distribution Function as a Function of Extruder Conditions	49
Figure 4.23	Residence Time Distribution Function as a Function of Extruder Conditions	50
Figure 4.24	Mean Residence Time as a Function of Barrel Temperature	50
Figure 4.25	Concentration of the Tracer Components versus Time	52
Figure 4.26	Loss of Tracer Components at Steady State Extruder Condition	52

LIST OF TABLES

		PAGE
Table 2.1	Physical Properties of BP and TAC	8
Table 2.2	Molecular Transitions and Energy Requirement	14
Table 3.1	Details on the Polymer Used	25
Table 3.2	List of the Chemicals Used	25
Table 3.3	Properties of the Silicone Oil Used	25
Table 3.4	Extrusion Conditions of the Three-Factorial Experimental Design	29
Table 3.5	Extruder Conditions for Input Additive Concentration Variation Experiments	29
Table 3.6	Extruder Conditions for Stimulus Response Technique Experiments	34
Table 4.1	Physical Characteristics of Additives Mixtures	35
Table 4.2	Additives Distribution along the Extrudate	39
Table 4.3	Statistical Analysis of Factorial Design	40
Table 4.4	Analysis of Variance Table for Loss of Benzophenone	41
Table 4.5	Analysis of Variance Table for Loss of TAC	41
Table 4.6	Mean Residence Time and Extruder Deadvolume Fraction	51
Table 4.7	Processing Conditions and Results of Additive Incorporation with the High-Intensity Internal Batch Mixer	53
Table 4.8	Average Total Additives Loss and Average Total %wt. Additives Incorporated with the High-Intensity Internal Batch Mixer	53

1. Introduction

Polyethylene is one of the most commonly used synthetic polymers. The use of polyethylene is greatly restricted by creep (the gradual deformation of material under a constant load over time).

In the last years, radiation has been applied to cross-link polyethylene in order to improve its mechanical properties [1-5]. Recognized by Oster [6, 7] UV cross-linking of polyethylene has been investigated over the last 50 years [8-21].

The polymer orientation-crosslinking process involves extrusion followed by melt drawing and finally cross-linking. The product is a low-creep high-strength plastic wire. A combination of two additives are used in this process: benzophenone (BP) creates free radicals when exposed to ultraviolet light and tri-allyl cyanurate (TAC) greatly assists cross-linking of the polymer molecules.

Two aspects of these materials provided the motivation for this work: TAC is not free flowing at room temperature and the usual plastic wire extrusion temperature may exceed the boiling point of the additive.

Thus, the objectives of this work were:

- to devise a continuous method for incorporating crosslinking additives into the polymer orientation-crosslinking process;
- to develop Fourier Transform Infrared spectroscopy methods which can provide both the average concentration of additives in the wire and the variation of concentration across the diameter of the wire;
- to examine the effect of processing variables on additive concentration with emphasis in determining the source of additive losses during processing.

2.0 THEORETICAL ASPECTS

2.1 Overview

Developing a continuous method for incorporating of crosslinking additives in the polymer orientation-crosslinking process is central to all objectives of this work. Section 2.2 details the aspects of additives incorporation in the polymer processing which are particularly relevant here.

In accord with the second objective, section 2.3 describes pertinent details about Fourier Transform Infrared spectroscopy.

Section 2.4 refers to the last two objectives: effect of processing variables on additive concentration and investigation of the source of additive losses .

2.2 The Polymer Orientation-Cross-linking (POC) Process

Figure 2.1 shows a schematic of the POC Process. High density polyethylene (HDPE) together with two additives (a photoinitiator and a cross-linker) are fed into a single screw extruder. When the polymer mixture exits from the die it is stretched to obtain orientation and is then cross-linked using uv irradiation to “lock-in” the orientation. The result is a low creep, high modulus plastic wire. An early version of this process was developed by Ranby et al. [22-30]. A newer version of the process includes orientation during as well as previous to the cross-linking stage and is the one used here [31].

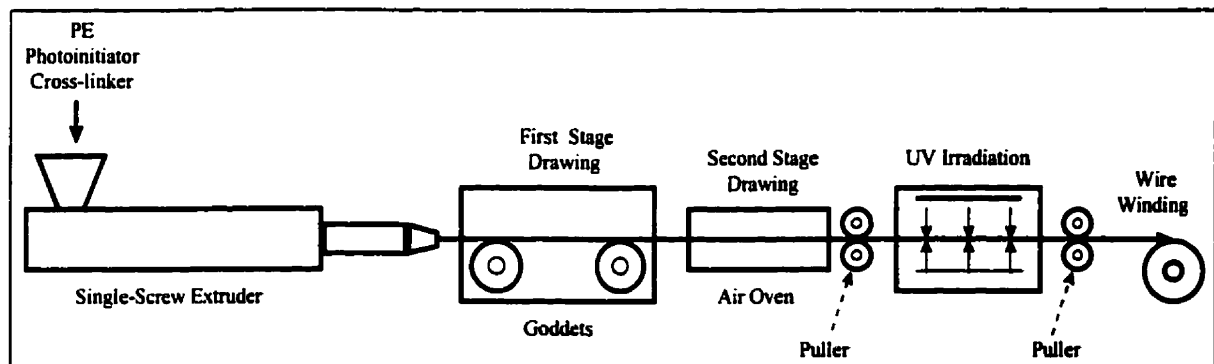


Figure 2.1: Schematic of PCO Process

Polymers are long chain molecules of carbon atoms covalently bonded together . They consist of repeating subunits (monomers), where the main chains are held together by secondary (e.g. Van der Waals) bonds. Polyethylene is the simplest of all polymers. It consists of repeating ethylene units ($-\text{CH}_2-\text{CH}_2-$) and possesses a semi-crystalline morphology, which is characterized by alternating crystalline and amorphous regions. Polyethylene is most commonly characterized by its molecular weight and its branching characteristics. The molecular weight is expressed in terms of molecular weight distributions or distribution averages such as the number average molecular weight (M_n), weight average molecular weight (M_w), and polydispersity (PD) (the ratio of M_w to M_n). Polyethylene is classified according to its branching characteristics into high density (HDPE), linear low density (LLDPE), and low density (LDPE) polyethylene.

Since incorporation of the two additives into the polyethylene forms the central topic of this thesis the role of the additives in the process will be more fully discussed in the following paragraphs.

Photoinitiators are monomers that absorb ultraviolet light energy in the spectral range from 250 to 400 nm and convert it into chemical energy by the formation of reactive intermediates [32] which in turn produce macroradicals by abstracting hydrogen atoms from the surrounding molecules or adding to double bonds.

The photoinitiators can be divided in two groups: those which undergo photofragmentation into other species (e.g., hexachlorobenzene) and those which abstract hydrogen in the excited state (e.g., benzophenone and its derivatives) [24]. To initiate cross-linking of PE, it is essential that either the radicals formed in the fragmentation reaction or the excited state of the hydrogen abstracting type photoinitiators must be able to abstract hydrogen from polyethylene chains or add to double bonds with sufficient efficiency to produce macroradicals. BP the photoinitiator used in this study is known to be highly effective in hydrogen abstraction [7, 32, 33]. It has two spectral absorption peaks respectively at 254 nm and 337nm. As shown in Figure 2.2 when exposed to these wavelengths, BP is excited to a singlet state (S_1) which rapidly converts into an excited triplet state (T_1) by intersystem crossing with 100% efficiency (see Jablonski diagram in Appendix I). The excited triplet

state (T1) presents long-living diradicals which readily abstract hydrogens from the surrounding polymer molecules, forming reactive free radicals along the polymer chains.

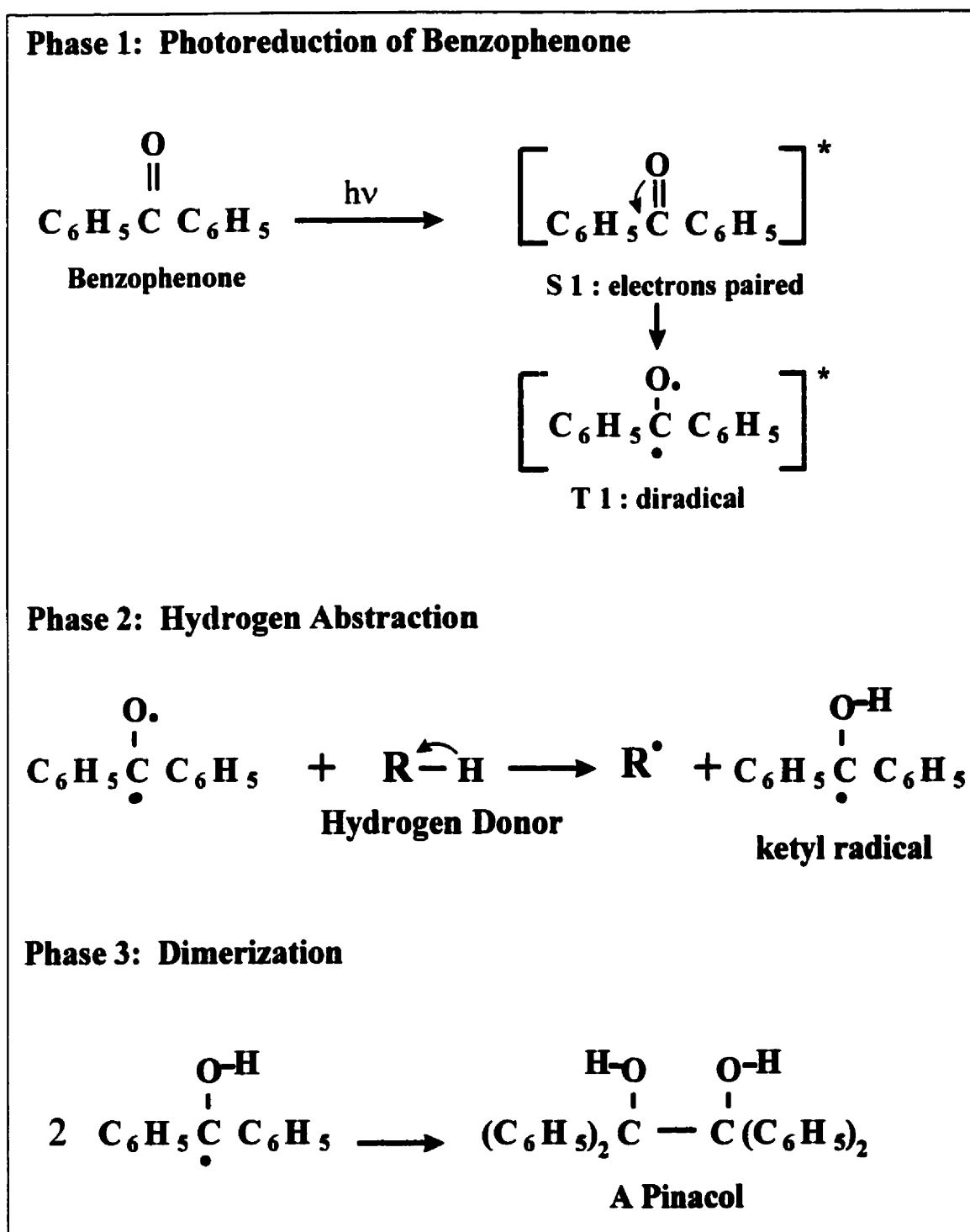


Figure 2 2: Reactions of Benzophenone to Ultraviolet Radiation.

Figure 2.3 from Ranby et al.[24] shows how the amount of cross-linked gel increases as the amount of BP used increases. Note that the amount of gel formed tends to level off at higher BP concentrations. For use of a specific photoinitiator, factors as efficiency, chemical stability, solubility, compatibility, toxicity and color are most frequently considered.

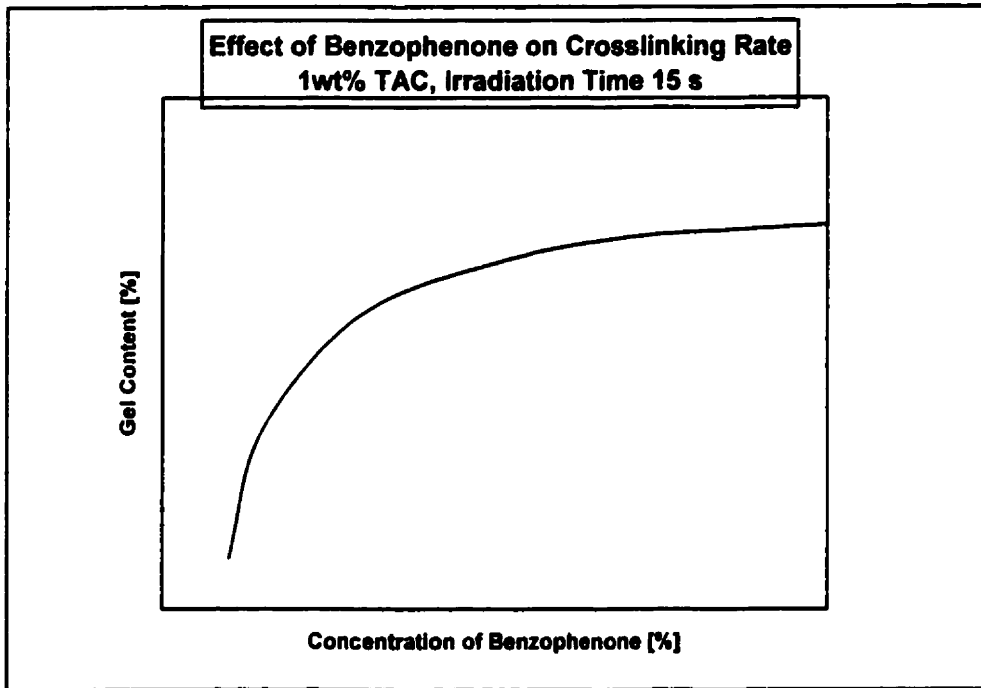


Figure 2.3: Effect of Benzophenone on Crosslinking Rate

Cross-linking agents are reactive, multi-functional organic monomers, usually allyl ethers or acrylates with two or more double bonds readily forming radicals. The cross-linking agent shown in Figure 2.4 is the second additive whose presence is very important for cross-linking process, TAC. TAC adds to the active site produced by the photoinitiator to provide a bridge between the polymer molecules. Figure 2.5 shows the main reactions of TAC. The allylic hydrogens of TAC are readily abstracted by the excited triplet state of the photoinitiator forming TAC-allyl radicals (reaction #3). The alkyl radicals on PE-chain can add to the double bonds of TAC initiating its polymerization (reactions # 6). The TAC-allyl radicals formed are relatively stable and their combination has been proved to be the main crosslinking route (reactions #7 through 11 of Figure 2.5).

As shown in Figure 2.4, TAC accelerates the rate of cross-linking of PE.

Photochemical TAC monomers are grafted on PE chains and participate in forming cross-links. TAC molecules, being bonded to the macroradicals, do not increase the number of the latter but do alter their structure. It is clear that if a starting macroradical is susceptible to destruction, at branch points or in stressed segments for example, the TAC attachment should prevent a break of the chain and the macroradical formed will have a higher probability of participating in the recombination process to form a cross-link.

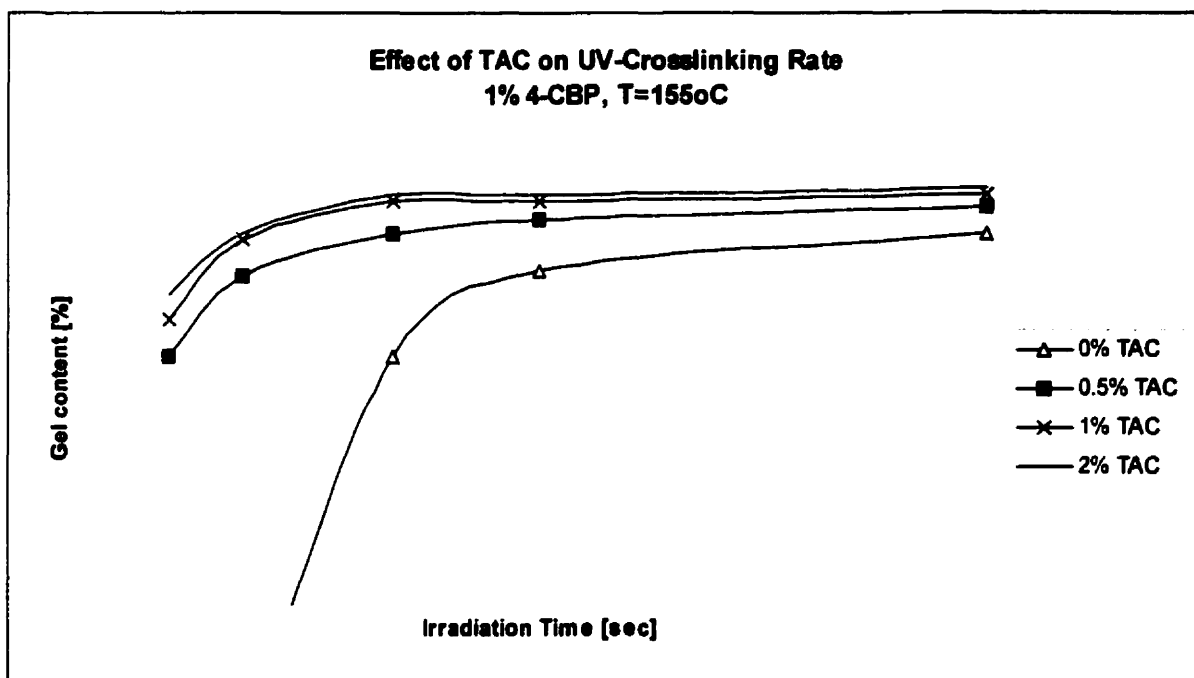


Figure 2.4 : Effect of TAC on Crosslinking Rate (Bengt Ranby)

In the POC process the addition of TAC as crosslinker greatly increases the depth of penetration of the crosslinking reaction. This is evident in Figure 2.6 where the homogeneity of crosslinking of the product is shown to be greatly improved by the addition of TAC.

Ranby and associates [24] propose crosslinking mechanism shown on Figure 2.5 :

(1) Hydrogen abstraction by excited triplet state of photoinitiator (PI)* :



$P = PE$ molecule, $P\bullet =$ alkyl radical on PE chain, $P\bullet^{\prime} =$ allyl radical on PE chain.



$T\bullet =$ TAC allyl radical; $PT =$ intermediate formed by $P\bullet^{\prime}$ and $T\bullet$.

(2) Combination and Polymerization:



$PT_{\bullet n} =$ propagating radical

(3) Cross-linking:



Figure 2.5: The Main Reactions of TAC and the Photo-cross-linking of Polyethylene

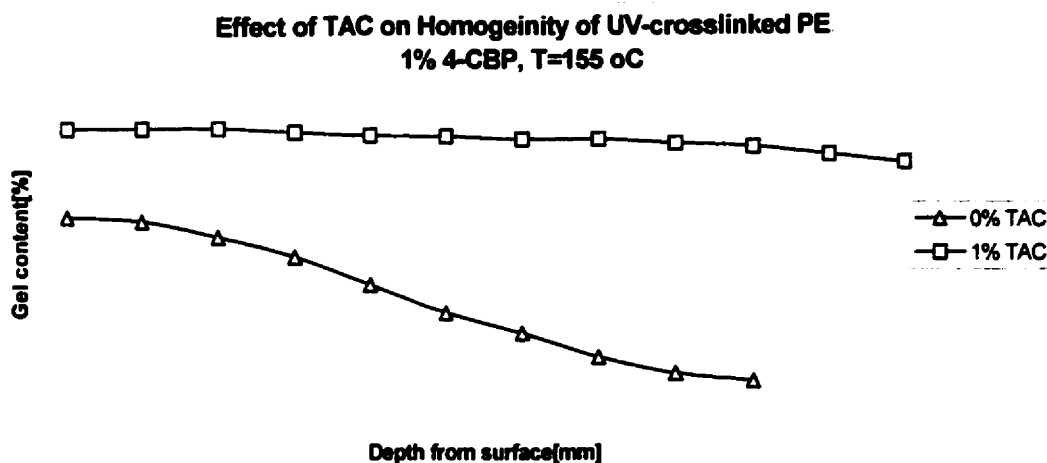


Figure 2.6: Effect of TAC on Homogeneity of UV-crosslinked PE (Bengt Ranby)

Physical properties of the two additives is shown in Table 2.1. It can be concluded from Table 2.1 that BP and TAC are low melting point additives.

Additive	Melting point [$^{\circ}$ C]	Boiling point [$^{\circ}$ C]
Benzophenone	48.1	305.0
TAC	26 -28	212

Table 2.1: Physical Properties of BP and TAC

2.2.1 Methods of Introducing BP and TAC

The first objective of the work is to devise a method of introducing the additives TAC and BP into the plastic wire process. Two methods were considered:

- pre-extrusion dry blending
- direct feed as individual streams into the extruder during processing.

These are discussed in turn below.

2.2.2 Dry Blending

Dry blending of additives into polymer previous to extrusion is widely practiced. However, it is known that differences in particle size, density and shape can impair blending effectiveness or even cause complete segregation of the components during blending. Dry blending of components with a particle size difference more than a factor of four results in segregation [34-38]. In exceeds, substantial differences in viscosity also cause segregation : in practice polymer pellets are not blended with liquid additives, a participation of more than 7% of a liquid component in blending of granular polymers results in segregation [34-38] [Granular polymers are polymer forms which particles have very rough surface and size less than 1 mm]. Also, electrostatic effects can affect blending. One method used in attempt to overcome the heterogeneity resulting from such effects is master-batching. In master-batching a high concentration of additives is blended into the polymer and extruded. Then, this concentrated product is "let-down" (i.e. diluted) in a second extrusion step[34-38].

Previous work in the POC process has employed dry blending without master-batching. A stirring mixer was used in an attempt to improve heterogeneity [22, 23, 26]. LDPE in powder or granules was mixed with BP and TAC before they were fed into the extruder. In the work of Ranby and associates [22 and 23] LDPE granules were mixed with desired amounts of additives (BP and TAC) in a powder mixer before being fed into a twin-screw extruder "Brabender". The "Brabender" performed functions of melting, melt mixing, and extrusion. The melted compound was extruded through a slit die and the extrudate (a ribbon-shaped profile) was stretched by a conveyor and UV-cross-linked simultaneously or separately. No data about parameters of pre-extrusion dry blending and output additive concentration were published. An other approach of the same research group included the use of a high-intensity batch mixer with and without pre-extrusion dry blending [24, 26]. Only BP was involved in pre-extrusion dry-blending [26]. TAC, because of its low melting point at 28°C was fed directly to the high-intensity batch mixer "Brabender" where the additive incorporation was conducted in 10 minutes at temperatures of 170-200°C. The mixture was then pressed at 170 °C into 2 mm thick plates and UV-irradiated. No pre-extrusion dry blending parameters were considered. In all previous work the loss of additives

during processing and the homogeneity of the product were not investigated: the input additive concentrations were accepted as equal to the output additive concentrations.

2.2.3 Direct Feed

Benzophenone and TAC are solids at room temperature. It was decided to investigate the possibility of depressing the freezing point of the TAC by adding benzophenone to it. If the two additives are mutually soluble and the freezing point could be depressed below room temperature, then the TAC and benzophenone together could be pumped into the process as a liquid.

Consider the behavior of two-component systems in which equilibrium exists between a solid and a liquid phase only (Figure 2.7) [39]. Component A and component B are completely miscible in the liquid state in all proportions. Since only the pure components can occur as solid phases, the only systems possible are S_A-L , S_B-L , and S_A-S_B-L where S_A and S_B represent the solid components and L the liquid solution. Under given pressure the equilibrium is represented by a temperature-concentration diagram. In the simplest possible equilibrium diagram for a two-component system solid solutions are not formed, the points A and B then represent the melting points of the pure components. Since the freezing-point of a liquid is lowered by dissolving another substance in it, it follows that if a quantity of the component B be dissolved in molten component A, the temperature at which solid A will be in equilibrium with the solution will be below the freezing-point of pure A. The greater the concentration of component B in the liquid, the lower will be the temperature at which A can exist in equilibrium with it.

The curve AC represents the composition of solutions which are in equilibrium, at different temperatures, with the solid component A; and the curve BC- the composition of solutions in equilibrium with solid component B. At the point C, where the two-curves intercept, both solid components can exist in equilibrium with a liquid solution of definite composition, corresponding with the point C. Point C is called a eutectic point. It lies at a lower temperature than the melting-point of either component.

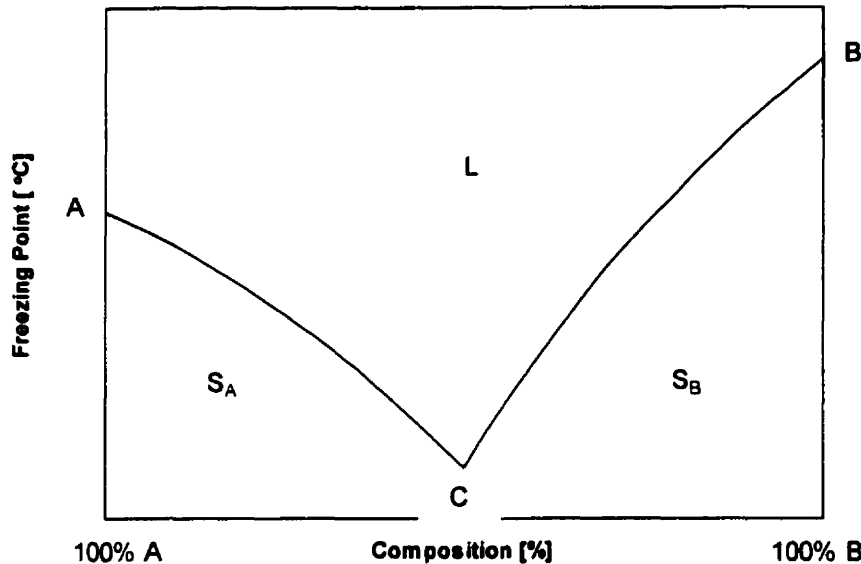


Figure 2.7: Phase Equilibrium Diagram of Two Component System

2.2.4 Basic Aspects of Additives Incorporation

Each additive system can be most efficiently incorporated into the polymer by performing the mixing operations at conditions of most similar viscosity. To carry out the process objectives successfully, a compounding machine with excellent conveying characteristics is essential. Maximum flexibility in location of feed inputs is also very important. Without this flexibility it may be necessary to sacrifice material quality in order to compound at high levels, or lower level of additive incorporation may have to be accepted. The ability to specify exactly where and how much shear input will be located within the processing section and the ability to control the degree of mixing intensity by using different screw hardware combinations are invaluable in the compounding of polymers with additives. The equipment for compounding additives into a polymer system must be capable of performing some of the following process tasks:

- incorporation and homogenization of additives without exceeding degradation temperatures;
- generation of high shear stresses (for good dispersion);

- homogenization of two or more materials of different melt viscosity without resulting in a stratified or layered final mix ;
- provision of uniform shear stress and heat history to each particle;
- provision of precise control over the process to ensure narrow temperature distribution throughout the process and at discharge.

The low melting point additives present problems when compounded for master batching [38]. They melt before the polymer has become molten and act as excellent lubricants. This presents a conveying problem in conventional compounding equipment, which can be overcome by the use of intermeshing twin-screw extruders with their positive conveying characteristics. The viscosity differences present obstacles to effective melting and homogenizing. To achieve effective homogenization, the components should have nearly equal viscosity. This can best be achieved for liquid additives when the polymer is fully molten. By injecting the liquid additive downstream into the processing section after the polymer melting has taken place, high levels can be incorporated and homogenized in this type of compounder. Kneading elements effectively introduce high amount of energy at specific locations within the processing section. These kneading elements, also by changing their shear direction, overcome the striation problem inherent in less sophisticated mixing equipment.

Among the variety of twin-screw designs the two basic types which are widely used for compounding operations are intermeshing counter-rotating and intermeshing corotating twin-screw machines. An analysis of the velocity and stress distribution of the both types shows that the degree of uniform dispersion is directly related to stress/strain distributions, particularly at low concentrations. The conveying efficiency is superior to that possible in single-screw machines. Good control over residence time distribution is an essential feature of a continuous compounding system. The residence time distribution must be short and uniform to minimize heat history.

2.3 Analysis of Additive Concentration

The second objective of this work was to develop a Fourier Transform Infrared Spectrometer (FTIR) method of measuring both the average additive concentration and their

concentration profile across the diameter of the wire. FTIR spectroscopy is a powerful, infrared technique which analyzes the sample beam at all wavelengths simultaneously, rather than individually [40-55]. FTIR was selected after careful consideration of the many difficulties associated with additive concentration measurement. These difficulties include: the insolubility of the polymer matrix, additive insolubility (elevating the temperature during sample preparation can change the concentration and the presence of combinations of additives as well as additive degradation products). FTIR can potentially overcome all of these difficulties. Furthermore, it operates in either a transmittance or reflectance mode (and thus accommodate opaque samples).

FTIR microscopy can enable a concentration profile to be obtained since it can provide the spectrum of a 10 μm diameter spot. In the next section, the principles of FTIR and FTIR microscopy are described with emphasis on sources of error in the methods. The following section shows typical spectra for the additives used here and the quantitative methods involved.

2.3.1 Principles of FTIR and FTIR Microscopy

The electromagnetic spectrum (EMS) consists of radiations of varying wavelengths as shown in Figure 2.8:

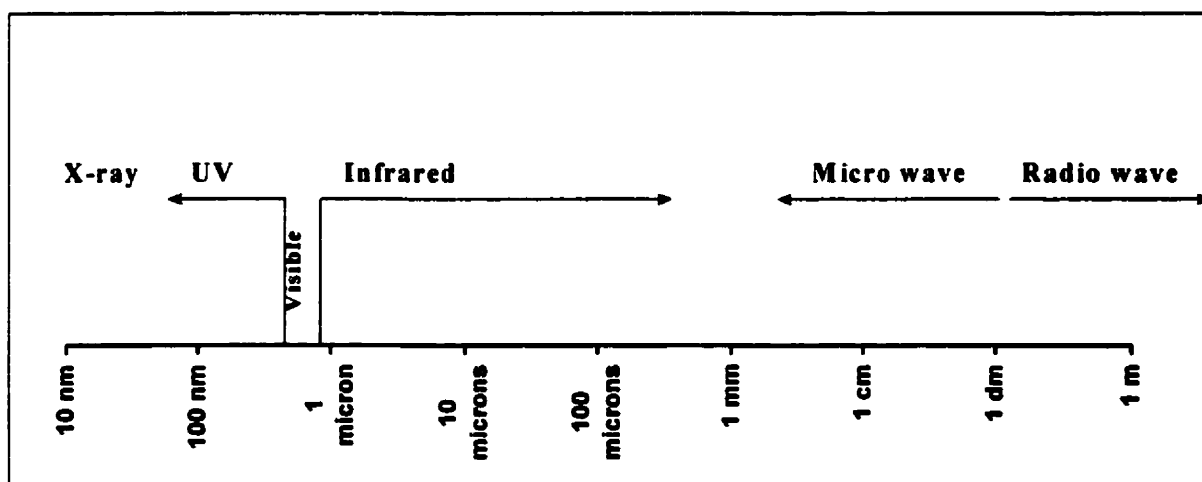


Figure 2.8: Entire Electromagnetic Spectrum

Energy is transferred as quanta of discrete magnitude (photon). The quantum or energy of a particular electromagnetic radiation is a function of frequency.

$$E = h\nu$$

where:

h = Plank's constant

ν = the frequency of radiation

Matter (atoms, ions or molecules), when irradiated with light, absorbs or emits energy according to the rules of quantum mechanics, which stipulates that energy transfer takes place in quanta of definite energy. The magnitude of the quanta is characteristic of the specific molecule.

Energy is absorbed by the molecule to affect a transition from a lower energy level to a higher energy level. Since matter is more stable at lower energy levels, the 'excited molecule' will try to return 'ground state'. As the molecule passes down the energy levels, the release of quanta in either single or in multiple steps will occur. This results in the emission of energy.

For a particular transition to occur, energy must be supplied in exact amounts (quanta). If the energy supplied is smaller than the required quantum, transitions corresponding to lower energy levels will takes place. However, if the energy of the quantum supplied is higher than what is actually required for a particular transition, then higher order transitions will takes place. By monitoring the amount of energy absorbed or emitted by a given material in a range of frequencies, the chemical structure can be elucidated.

Vibrational Energy Levels

The change in energy of a molecule is seen in Table 2.2:

Energy Transitions	EMS Range	Energy Needed (kcal/mol)
Electronic	UV/VIS	100
Vibrational	IR	5
Rotational	far-IR/microwaves	0.001

Table 2.2: Molecular Transitions and Energy Requirement

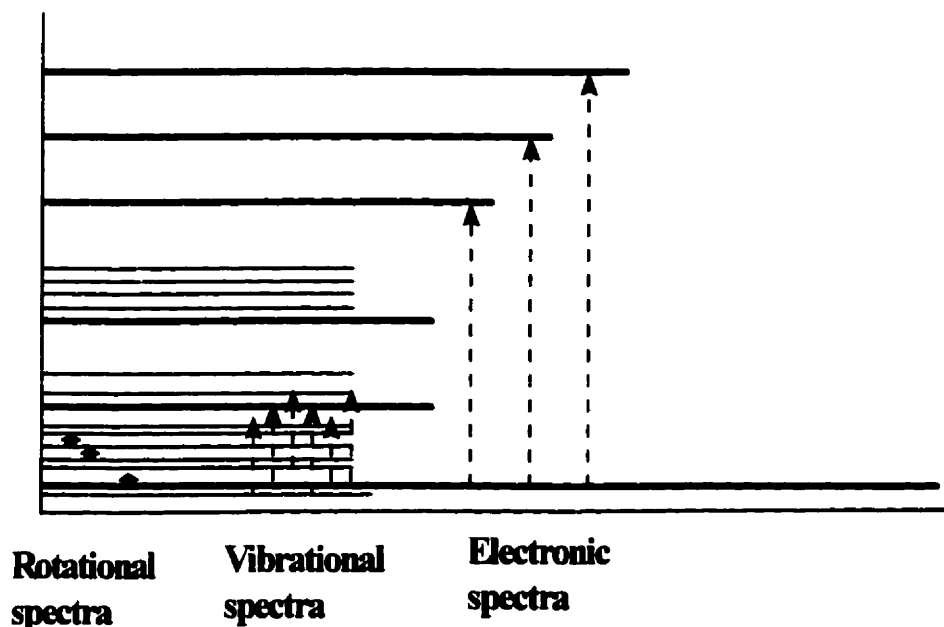


Figure 2.9: Schematic of Molecular Energy Levels

As illustrated by Figure 2.9, each vibrational level has a set of rotational levels associated with it while each electronic level has a set of vibrational levels. This overlap between the energy levels of electronic, vibrational and rotational energy levels are due to the additive properties of the quanta. Vibrational and rotational motions can occur only in polyatomic systems, so that IR spectra are produced only by molecules.

It was already seen that IR spectra results from the absorption or emission of IR radiation by the molecule. For IR absorption to occur:

- a) the energy of the radiation must coincide with the energy difference between the excited and ground states of the molecule (i.e., quanta must match) and
- b) the vibration must entail a change in electrical dipole moment of the molecule.

The same molecule can exhibit different types of vibrations, depending on the number of atoms participating in the vibration and the structure of the molecule. For example, the two C-H bonds in a methylene group can undergo about six types of vibrations as shown in Figure 2.10 below:

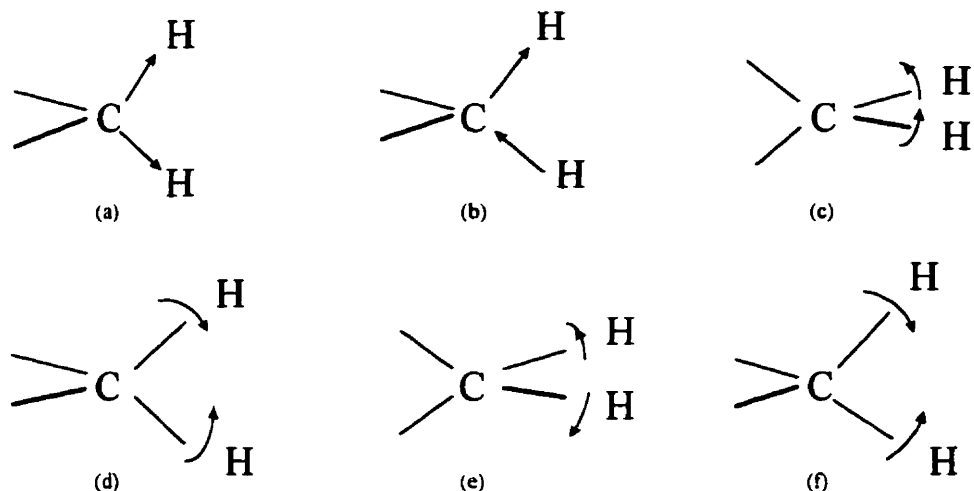


Figure 2.10: Vibrational Modes of C-H Bonds in Methylene group

- (a) symmetrical stretching;
- (b) asymmetrical stretching;
- (c) wagging or out-of-plane bending;
- (d) rocking or asymmetrical in-plane bending;
- (e) twisting or out-of plane bending;
- (f) scissoring or symmetrical in-plane bending.

The vibrations are classified as stretching or bending vibrations. Stretching vibrations occur when the participating atoms move along the axes of the bonds so the distance between the atoms change rhythmically. This is analogous to a spring. These vibrations can be symmetrical or asymmetrical with respect to a central atom depending on the direction of the stretching vibrations. The second type is a bending vibration in which there is a change in angle between the participating atoms. Complicated motion of atoms participating in a normal vibration make its frequency less characteristic. In this sense, stretching vibrations are more characteristic than bending vibrations, where, owing to various possible vibrations differing only slightly in frequency, it is difficult unequivocally to assign the band observed to such vibrational modes.

The bonds and atomic groups have characteristic modes of vibration. These can be determined mathematically for simple, symmetric molecules. Based on the nature of the

participating atomic nuclei, the symmetry of the molecule and the species of vibration, IUPAC has designed a system of designation. However this system of designation is not suitable when complex, asymmetrical molecules are to be designated. More details about some of the commonly encountered modes of vibration are provided in Appendix VI.

In addition to the fundamental modes of vibrations, there are overtones due to the involvement of neighbouring vibrating group. Two important classes of overtones are: harmonic overtone vibrations and combination bands. The harmonic overtone vibrations exist if the molecules possess a frequency that is a fraction of the fundamental frequency at a certain quantum level. Where as, a combination band is the sum or the frequencies of two or more fundamental or harmonic vibrations. In most of the applications these overtones are not very significant because their intensities are usually one-hundredth of those of fundamental bands.

The intensity of the IR absorption band is proportional to the rate of change of dipole moment with respect to the displacement of the atoms. As inherent dipole moments are generally stronger than induced dipole moments, groups such as -OH, -NH with strong dipole moments generally give strong absorption bands. In spectral analysis, it is common to classify the peaks according to their intensity in to very strong, strong, medium and weak peaks.

Infrared spectra of PE, BP, and TAC and their infrared wavelength characterization are given in Appendix III. Examination of this data shows that characteristic group frequencies particularly useful for quantitative FTIR-analysis of BP and TAC in PE are:

- Carbonyl group stretch at 1666 cm^{-1} (BP);
- C-H in plane banding at 1281 cm^{-1} (BP);
- C-H out of plane banding at 694 cm^{-1} (BP);
- Aromatic ring at 639 cm^{-1} (BP);
- Triazine-quadrant stretching at 1564 cm^{-1} (TAC);
- Triazine-out of plane bending at 820 cm^{-1} (TAC);

2.3.2 Quantitative FTIR Analysis

Beer-Lambert's Law

In infrared spectroscopy, IR radiation is irradiated on a sample and the spectrometer records the frequencies and intensities of the sample. The intensity of absorption is related to the concentration of the sample present as governed by Beer's Law.

$$A(\nu) = a(\nu) bc$$

where,

$A(\nu)$ = absorbance at wavenumber ν

$a(\nu)$ = molar absorptivity at wavenumber ν

b = path length

c = concentration

For a mixture of N components, the total absorbance at ν is given by:

$$A(\nu) = \sum_{i=1}^N a(\nu)bc_i$$

where, the subscript (i) refers to the i^{th} component of the mixture and N is the total number of component present.

Beer's law can be used for quantitative analysis in polymer-additives mixtures by using a calibration equation, which is obtained by: collecting FTIR spectra of different known concentrations of the additives in a relevant solvent, measuring the height (or calculating the area) of the relevant peaks and fitting an equation to the data plotted as height (or area) versus additive concentration.

Source of Errors in FTIR Spectroscopy

Fourier transform infrared spectrometry exhibits effects that may lead to errors in quantitative analysis. Some of these effects are inherent to FTIR spectrometry and others

pertain to IR spectrometry in general. One of the effects that is restricted to FTIR spectrometer performance is the stability of the interferometer. Instability in the interferometer may cause frequency shifts in spectra.

Instability in an interferometer may be classified into three broad types. First, there is short-term instability such as that due to mirror velocity fluctuations, mirror misalignment and the effect of mirror tilt. The effect of mirror velocity errors is to produce ghost peaks in the spectrum, and a poor mirror drive (tilt) degrades the resolution. These effects can be recognized by comparing spectra produced by the instrument with standard spectra. In quantitative analysis, these errors will produce anomalies from which incorrect conclusions may be drawn.

Medium-term fluctuations occur on a scan-to-scan basic. Because, these fluctuations are either cyclic or random in nature, they are not particularly important for quantitative work. These fluctuations have been studied in detail by de Haseth [54].

Long -term fluctuations can be exhibited by drifts in the system that occur over several hours. These fluctuations are important when two signal-averaged spectra are collected at different times and a drift or error has been introduced into the interferograms. The resulting spectra may have the wave number positions of peaks slightly offset, which can introduce photometric errors in difference spectra.

We are concerned with the error in the predicted concentration when using a calibration curve determined by linear regression.

The advantages of using FTIR over other methods of analysis are as follows:

- a) a small sample size can be used (10 to 15 μ m)
- b) detailed chemical bonding information can be obtained
- c) specific molecules can be identified
- d) the method is non-destructive
- e) analysis of surfaces can be performed in attenuated total reflection (ATR) mode.

2.4 The Effect of Processing Variables on Additive Concentration

The third objective of this work was to investigate the effect of processing variables on additive concentration. A homogeneous dispersion of BP and TAC across the diameter of each extruded strand as well as lengthwise along each strand was desired. In addition, additive loss was to be minimized. As shown in Figure 2.11, the actual POC process used here involved a pre-processing extrusion step to obtain pellets containing well dispersed additives:

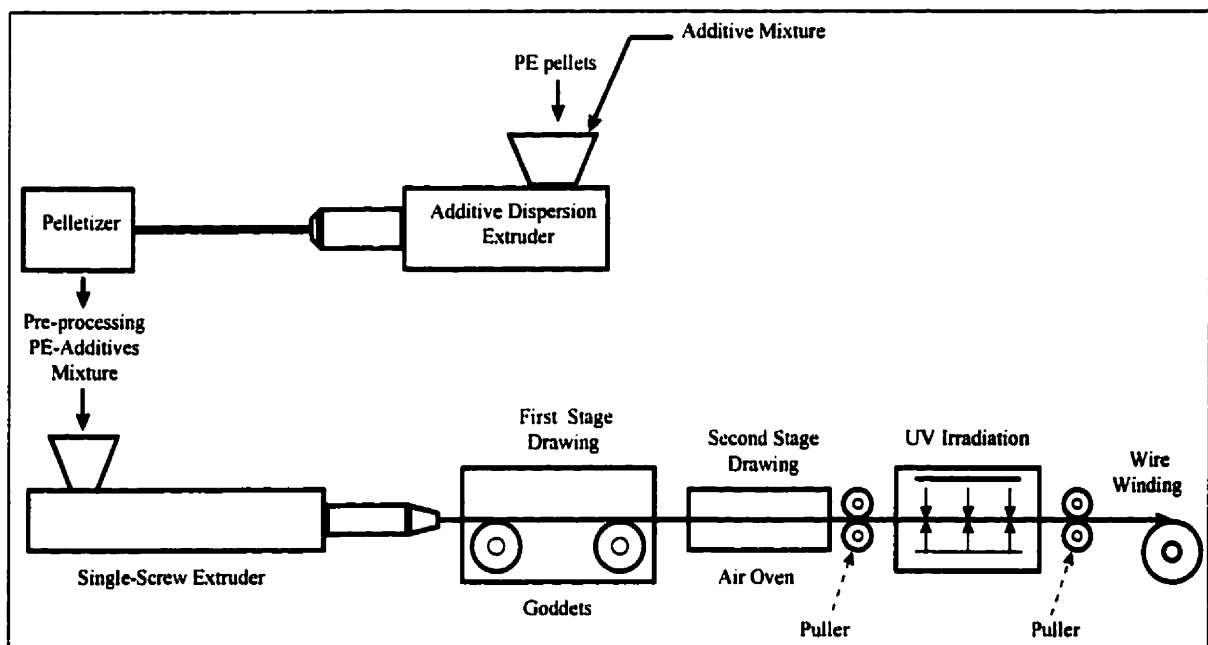


Figure 2.11 : Schematic of Polymer Orientation-Crosslinking Process

The whole thesis focuses upon that extrusion process and the extruder employed will be referred to as the “Additive Dispersion Extruder”. Further details may be found in the Experimental section. At this point it must be pointed out that the Additive Dispersion Extruder, unlike the one used to feed the orientation equipment, was a very short, twin screw machine with counter-rotating, inter-meshing screws. As mentioned above, twin screw extruders are well known for having some positive displacement action (they more closely resemble positive displacement pumps than do single screw extruders). While mathematical analysis of the flow in single screw extruders is very advanced, analogous analysis of flow in

twin screw extruders is much more difficult and therefore much less developed. The most common method of characterizing mixing in twin screw extruders is by the use of residence time distributions. The next section presents the main equations associated with residence time distributions. The following section discusses the problem of additive loss and proposes a method of using residence time distributions to assess the significance of additive evaporation.

Residence Time Distributions

This information on the distribution of ages of molecules in the exit stream or the distribution of residence times of molecules within the vessel can be found by a widely used stimulus-response technique. The information obtained can then be used in one of two ways to account for the non-ideal flow behavior of fluid in a chemical flow reactor.

If a small quantity of a dye is injected as a sharp pulse into the feed port of an extruder, the concentration of dye in the output polymer measured as a function of time since the injection is termed a residence time distribution. The distribution discloses the variety of residence times in the extruder represented in a sample from that equipment.

The use of residence time distribution study as an analytical tool for continuous flow processes is generally attributed to Danckwerts [56, 57]. He considered a steady-state flow of a single fluid through a vessel, without reactions and without density change.

The mean residence time is defined by:

$$\bar{t} = V / v \quad (1)$$

where V is reactor(extruder) volume and v is reactor (extruder) flow rate.

A dimensionless variable called reduced (normalized) time θ which measures time in units of mean residence time, is defined:

$$\theta = t / \bar{t} \quad (2)$$

The exact form of the equations which we used are given by Levenspiel [58]. The residence time distribution is calculated from experimental data as follows :

$$\text{Exit age distribution: } E(t) = C(t) / \int_0^{\infty} C(t) dt \quad (3)$$

where :

$E(t)$ is the exit age distribution function of a fluid leaving a vessel or the residence time distribution of a fluid in a vessel. $E(t)$ is a measure of the distribution of residence times of the fluid in a vessel.

$C(t)$ is the tracer concentration in the extrudate at time t .

If a step change in tracer concentration is effected in place of a pulse, then the resulting response is termed a cumulative residence time distribution $F(t)$ and is given by

$$\text{Cumulative distribution: } F(t) = \int_0^t E(t) dt = \int_0^t C(t) dt / \int_0^{\infty} C(t) dt \quad (4)$$

Age distribution functions can be expressed in dimensionless time units θ :

$$E(\theta) = \bar{t} \cdot E(t) \quad (5)$$

$$F(\theta) = \bar{t} \cdot F(t) \quad (6)$$

The mean residence time \bar{t} is given by the equation:

$$\text{Mean residence time: } \bar{t} = \int_0^{\infty} t C(t) dt / \int_0^{\infty} C(t) dt \quad (7)$$

The interrelating expressions between E and F are :

$$F(\theta) = \int_0^{\theta} E(\theta) d\theta \quad (8)$$

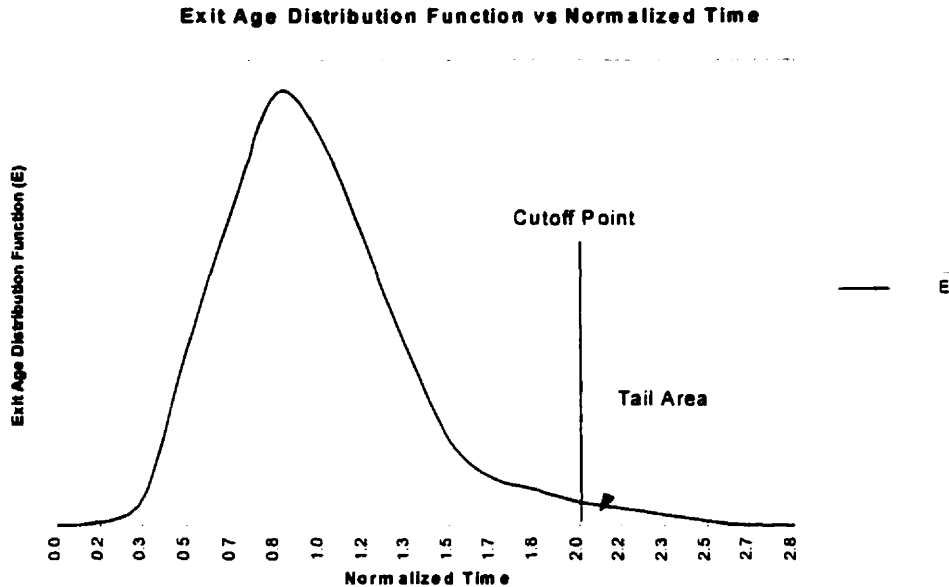
The measurement of residence time distribution of extruders has generally been done either by the use of tracers which could be detected by traditional analytical chemistry techniques or by radioactive methods. Examples of chemical tracers and their related

measurement are summarized with following paragraph:

Danckwerts [56] and Bigg and Middlehan [59] measured the presence of a red dye by light transmittance with a spectrophotometer. Todd [60] and Janssen [61, 62] report the use of methylene blue, also measuring the concentration by photospectrometer. Antimony oxide was used by Rauwendaal [63] and cadmium selenide by Walk [64] both using x-ray fluorescence as the detection means. Radioactive isotopes can be used directly as tracers, or suitable materials (such as MnO_2) can be extruded, and then subjected to neutron activation analysis. Wolf and White [65], Schott and Saleh [66], Janssen [61] have reported using these methods.

Another approach is to measure an electrical property of a tracer stream and relate that to concentration. Todd and Irving [67] measured conductivity of glucose solutions doped with KNO_3 or NaNO_3 . Werner and Eise [68] used an on-line technique to measure inductance of polyethylene melts doped with iron powder. Golba [69, 70] described a technique in which carbon black was used as a tracer in polystyrene melts.

Figure 2.12 shows how the residence time distribution functions can be used to determine whether or not there is a significant extruder deadvolume region. Integrating the area under the curve from the cutoff point selected as the time required to process two extruder volumes of polymer to the point where $E(\theta)$ falls to zero represents the fraction of what is considered extruder deadvolume.



**Figure 2.12 : Plot of Exit Age Distribution Function (eq.5) vs Normalized Time (eq.2)
Tail area represents the extruder deadvolume fraction.**

Additive Loss

The high vapor pressure of BP in the conditions of the extrusion process (high barrel temperature 160 - 200⁰C) may result in additive loss due to fast evaporation. In the POC process the barrel temperature of the extruder may exceed the boiling temperature of TAC which also may result in fast evaporation and significant loss of this additive.

Also, it would be expected that longer mean residence time (RPM) at elevated temperature may cause higher additives loss.

The die temperature also may have some effect on additive loss due to evaporation of the additive as it exits from high pressure to atmospheric pressure.

A tracer consisting of a non-volatile component together with the cross-linking additives can be used to assess the significance of additive evaporation. If a step change of the tracer input concentration is effected then the output concentration and loss of each tracer component can be observed. Comparison of the additive loss with the loss of the non-volatile component at steady state extrusion conditions provides an indication of the significance of additive evaporation.

3.0 EXPERIMENTAL

3.1 Materials

Details regarding the high density polyethylene (HDPE) used in this work are shown in Table 3.1. Table 3.2 shows details on the cross-linker and photoinitiator used.

HDPE	Manufacturer's Designation	Molecular Properties	MFI g/10 min	Density g/cm ³
FINA 7208	Fina Oil and Chemical	Mw = 138,000 ± 13,226 Mn = 32,780 ± 3,053	0.60	0.959

Table 3.1 Details on the Polymer Used

Trade Name	Manufacturer's Designation	General Name	Formula
Triallyl-Cyanurate (TAC) (Cross-linker)	Aldrich Chemicals Milwaukee, Wisconsin	2,4,6, Triallyloxy - 1,3,5, Triazine	C ₃ N ₃ (OC ₂ =C) ₃
Benzophenone (BP) (Photoinitiator)	Aldrich Chemicals Milwaukee, Wisconsin	Diphenyl ketone	[C ₆ H ₅] ₂ CO

Table 3.2 List of the Chemicals Used

Xylene (ACS Grade - Aldrich Chemical, Milwaukee, Wisconsin) was used as a solvent for FTIR analyses.

High-Temperature-Resistant Silicone oil (Aldrich Chemical) was used as a non-volatile tracer component for obtaining extruder residence time distribution functions. Its properties are summarized in Table 3.3:

Trade Name	Usable Range [°C]	Boiling Point [°C]	Density [g/ml]	Formula
High-Temperature-Resistant Silicone Oil	-40 to + 230	315	1.05	[(CH ₃) C ₆ H ₅ (SiO)] _n

Table 3.3 Properties of the Silicone Oil Used

3.2 Equipment

3.2.1 Additive Incorporation by Extrusion

Continuous melt blending of the additives into polyethylene was conducted with a C.W. Brabender, 1.5 “, laboratory, counterrotating closely intermeshing twin-screw extruder. The extruder was equipped with constant profile screws with an L/D ratio of 5:1. The extruder was electrically heated. Three controlled temperatures zones were present - two in the barrel and one in the die. A 4 mm outlet diameter die was used (See Figure 3.1).

The liquid additive mixture was delivered through the feed port directly into the intermeshing area of the screws by a high precision, LC-2600 syringe pump. The additive mixture was transported from the outlet of the syringe pump to the extruder through a plastic tube with a 1/16” inner diameter. To ensure a stable location of the additive insertion port, a stainless steel tube with a 1/16” inner diameter was used as the last section of additive pathway. The location of the additives insertion port is shown on Figure 3.1 and Figure 3.2

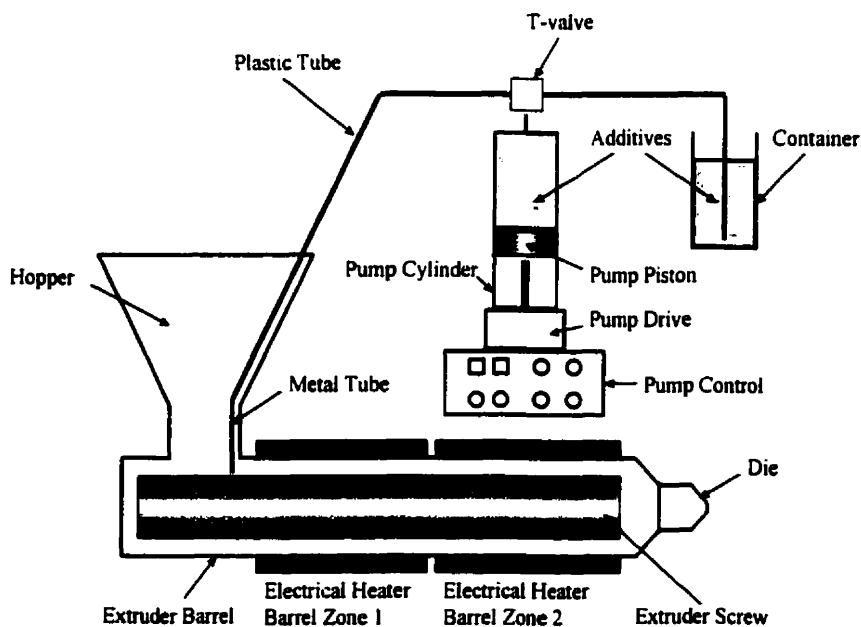


Figure 3.1: Schematic of the Extrusion System

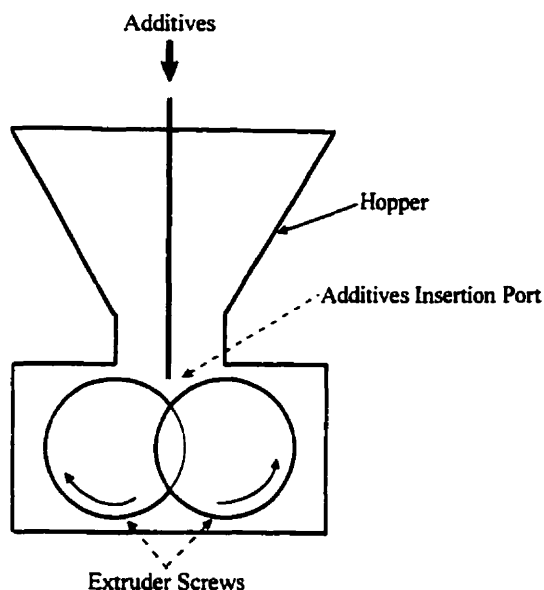


Figure 3.2: Schematic of the Location of the Additives Insertion Port

3.2.2 Additives Incorporation with a High-Intensity Internal Mixer

Batch mixing of additives was conducted with a C.W. Brabender , laboratory, non-intermeshing twin-rotor batch mixer. The mixer was electrically heated. The barrel temperature and the screw rotational speed were controlled. The mixer was equipped with a square feeding port with a closing device to prevent leaking of the mixer contents.

3.3 Experimental Procedure

3.3.1 Preparation of a Liquid Mixture of Cross-Linking Additives

150 g of Tri-allyl-cyanurate (Aldrich) (which at room temperature is a tacky solid) was heated at 45⁰C until completely melted and then benzophenone (Aldrich) was added. The mixture was stirred at 45⁰C for 15 min until benzophenone crystals were completely dissolved and the resulting product became a transparent and colorless liquid. The sample was then allowed to cool down at room temperature. TAC/Benzophenone mixtures containing 33 ; 43; 47 ; 50 ; 56 ; 67 wt% BP were investigated. The liquid specimens obtained were exposed to slow cooling and the temperature was measured

with a thermocouple. The temperature at which precipitation was observed was accepted as the freezing point.

3.3.2 Additives Incorporation by Extrusion

The additives were added using the high-precision displacement pump. The pump was filled with 250 ml liquid additive mixture (TAC / BP = 1 : 1) using the “Refill”-mode of the pump and a T-valve. Then by switching on the “Delivery”-mode of the pump and the T-valve the liquid additives mixture was injected into the small diameter hose already described in 3.2.1 until the hose was completely filled. Then the pump was turned on “Standby”-mode.

The extruder was heated for about one hour to equilibrate at the set temperatures. Then the hopper was filled with pellets and the system was allowed to run for half an hour to reach steady state conditions. Once steady state had been reached and the polymer mass flowrate obtained, the pump was set to the required flowrate setting and turned on “pump”-mode.

Two sets of experiments were conducted:

- a three-factorial design set of experiments where the extruder conditions were varied, but the input concentration of additives was kept constant. Extrusion conditions for the twin-screw extruder were set according to 3^2 factorial design and were summarized in Table 3. 4. The objective of the factorial design was to determine which extruder-processing variables were significant for the loss of cross-linking additives. The variables considered were: barrel temperature, extruder mean residence time and die temperature. The response variable was additive loss expressed as a percentage of the additive in the feed.
- the input additive concentration was varied but all other extruder conditions were kept constant. Experiments with 0.54, 1.04, 1.38, 1.84, 2.14, 2.22, 2.8 wt% input concentration of each additive were carried out The experimental conditions were summarized in Table 3.5.

File #	RPM [cm ⁻¹]	Temperature Profile [°C]			
		Barrel Zone 1	Barrel Zone 2	Die	Feeding Port
R1	2.4	140	160	160	90
R2	10	140	160	160	90
R3	2.4	140	160	190	90
R4	10	140	160	190	90
R5	2.4	140	200	160	90
R6	10	140	200	160	90
R7	2.4	140	200	190	90
R8	10	140	200	190	90

Table 3.4: Extrusion Conditions of the Three-Factorial Experimental Design

RPM [min ⁻¹]	Input Concentr. [wt%]	Temperature Profile [°C]			
		Barrel Zone 1	Barrel Zone 2	Die	Feeding Port
10	0.54	140	200	190	90
10	1.04	140	200	190	90
10	1.38	140	200	190	90
10	1.84	140	200	190	90
10	2.14	140	200	190	90
10	2.22	140	200	190	90
10	2.8	140	200	190	90

Table: 3.5 Extruder Conditions for Input Additive Concentration Variation Experiments.

3.3.3 Additive Incorporation by a High-Intensity Internal Mixer

The mixer was heated for about one hour to equilibrate at the set temperatures. Then 40 g of HDPE-pellets were added through the feed port and after a complete melting of the polymer 30 g liquid additives mixture (BP/TAC= 1:1) was injected with a syringe into the mixer. The process of mixing was observed through the feed port of the mixer. The system was allowed to run for 20 min at 60 RPM. Three sets of experiments were done with 3 replications each. The only variable was the barrel temperature. Runs were done at 160, 170 and 190°C. No leaking of additives was observed. After finishing of the experiments the mixer was disassembled and the specimens were collected and weighed.

3.4 Analytical Methods

3.4.1 Quantitative Fourier Transform Infrared Spectroscopy

Mid infrared spectra were obtained with a Mattson Galaxy GL-6020 FTIR spectrometer with an attached microscope. The light source was a He-Ne laser. The spectrometer was operated in the transmission mode. Samples were scanned 128 times with a resolution of 4 cm^{-1} from 400 to 4000 cm^{-1} . The instrument was equipped with a 5 mm diameter beam to scan large samples. In order to obtain maximum signal to noise ratio the microscope aperture was set to be 100 μm x 100 μm . Scans with the microscope were obtained in order to acquire quantifiable cross-sectional profiles using the x-y-z sample holder. The spectrometer was interfaced with a IBM 486-personal computer, equipped with a First Utility Matlab software package (Mattson Instruments, Madison, W.I.) used to collect and process the data. Spectral peaks were analyzed using the WinFirst software package (Mattson Instruments, Madison, W.I.).

Sample Preparation

Samples used in direct FTIR-analysis were prepared by cutting of the extrudate-rods into approximately 100 μm cross-sections using the Optical Lab microtome equipped with an inflexible blade. The quality of cutting was controlled by adjusting the

angle between the blade and the direction of motion of the sample holder. To prevent curling of the samples a polished though-steel lamella was used. The thickness of the samples was measured with a Mitutoyo, digital micrometer (Mitutoyo, Japan). The sample preparation technique is illustrated by Figure 3.3.

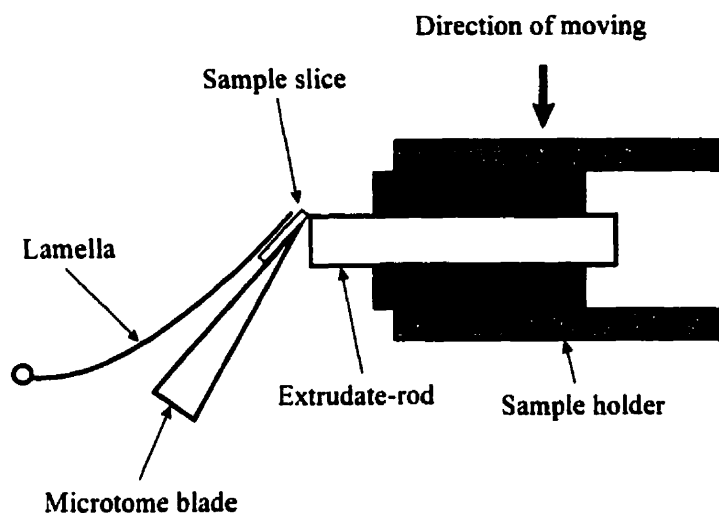


Figure 3.3: Schematic of Sample Preparation Technique

Calibration of TAC and BP

Quantitative analysis of BP and TAC in polyethylene was accomplished through calibration using IR-spectra of liquid solutions containing varying concentrations of TAC and BP. The advantages of this technique are:

- the concentrations of the calibrating samples were known with high accuracy. The error depended only on the accuracy of the weight-measuring equipment used.
- the possibility of losses during sample preparation (as existed when calibration was attempted by directly incorporating BP and TAC into PE) due to evaporation or migration were eliminated as the calibration samples were prepared at room temperature in closed vessels.

Concentrations of 0.20, 0.33, 0.53, 0.77, 1.3, 1.57, and 2.17 wt% of BP and TAC were dissolved into suitable solvent such as xylene which possessed no interfering absorbance

peaks relative to those additive peaks of interest. The solutions were injected with a syringe into a microflow cell (Graseby Specac, Fairfield, Connecticut). The microflow cell consisted of a 100 μm spacer, sandwiched between two 20 mm L x 10 mm W x 2 mm thick KCl windows. The height of the BP peak at 1666 cm^{-1} (C=O stretch) was used to associate absorbance to concentration and to obtain the molar extinction coefficient by using least square regression analysis. This peak was used in preference to the aromatic ring peak at 639 cm^{-1} (this peak has lower absorbance) and to the peak at 1281 cm^{-1} (C-H in plane bending) (this peak interferes with the TAC peak at 1328 cm^{-1} (C-O stretch)). With TAC the absorbance peak at 1564 cm^{-1} (triazine ring-quadrant stretching) was used in preference to the peaks at 1400 cm^{-1} (Triazine-semi-circle stretching), 1328 cm^{-1} (C-O stretch), 1138 cm^{-1} (O-CH₂ stretch) and 820 cm^{-1} (Triazine - out of plane bending). It provided a strong signal with higher precision, and no interference with another peaks. Spectra from pure xylene injected into a same microflow cell were used as a background for calibration curve data acquisition and subsequently subtracted to eliminate the error due to absorbance of solvent.

Spectra from pure polyethylene were used as a background for data acquisition of polymer samples containing additives and subsequently subtracted to eliminate the error due to absorbance of polymer. The thickness of the background-samples was chosen to match the thickness of the data-samples.

3.5 Residence time distribution

Tracer Preparation

100 g liquid additive mixture prepared the way described in 3.3.1 was added to 50 g high temperature resistant silicone oil. The mixture was stirred at room temperature for 10 min. The resulting product, a transparent, colorless liquid, contained TAC, benzophenone and silicone oil in equal weight ratio and was used as a tracer for obtaining extruder residence time distribution functions. The density of the tracer is 1.08 g/cm^3 and the boiling point is 308°C .

Tracer Experiments

Quantitative analysis of tracer in extrudate was accomplished through calibration using IR-spectra of Silicone oil, TAC and BP. Concentrations of 0.3, 0.6 and 1.25 wt% were dissolved into xylene. The solutions were injected with a syringe into a microflow cell (Graseby Specac, Fairfield, Connecticut). The microflow cell consisted of a 100 μm spacer, sandwiched between two 20 mm L x 10 mm W x 2 mm thick KCl windows. The height of the BP peak at 1666 cm^{-1} (C=O stretch) was used to associate absorbance to concentration. The absorbance peak at 1564 cm^{-1} (triazine ring-quadrant stretching) was used for TAC and the peak at 1260.4 cm^{-1} for Silicone oil.

Stimulus Response Technique Experiments

- **Pulse Tracer Input Signal**

0.16 g of the tracer was injected with a syringe as a sharp pulse into the feed port of the twin-screw extruder, running at steady-state conditions with pure polyethylene. After twenty minutes elapsed from the time of input tracer injection extrudate samples were collected every minute. The output tracer concentrations (output signal) were obtained using same techniques already described in Section 3.4.1. Two sets of experiments were done and are summarized in Table 3.6.

- **Step Tracer Input Signal**

0.576 g/min of the tracer was injected with a high-precision displacement pump into the feed port of the twin-screw extruder, running at steady-state conditions with pure polyethylene and extrudate samples were collected every minute. The extruder conditions were same as Run # RTD 4 in Table 3.6. The output tracer concentrations (output signal) were obtained using same techniques already described in Section 3.4.1.

Run #	RPM [min ⁻¹]	Temperature Profile [°C]			
		Barrel Zone 1	Barrel Zone 2	Die	Feeding Port
RTD 5	10	140	160	190	90
RTD 4	10	140	200	190	90

Table 3.6 Extruder Conditions for Stimulus Response Technique Experiments

4.0 RESULTS AND DISCUSSIONS

4.1 Development of a Continuous Method of Additive Incorporation

Results of the freezing point depression experiments are shown in Table 4.1 and Figure 4.1.

The main result was that a 50:50 mixture of BP and TAC was a mobile liquid with a freezing point well below room temperature (9°C). Continuous addition of the additives to the process involved simply metering the liquid into the extruder at the desired rate.

TAC/BP Ratio	Freezing Point [°C]	Boiling Point [°C]	Density [g/ml]
0	26	N/A	N/A
33	12	N/A	N/A
43	6	N/A	N/A
47	3	N/A	N/A
50	9	256	1.11
56	20	N/A	N/A
67	30	N/A	N/A
100	48	N/A	N/A

Table 4.1 Physical Characteristics of Additives Mixtures

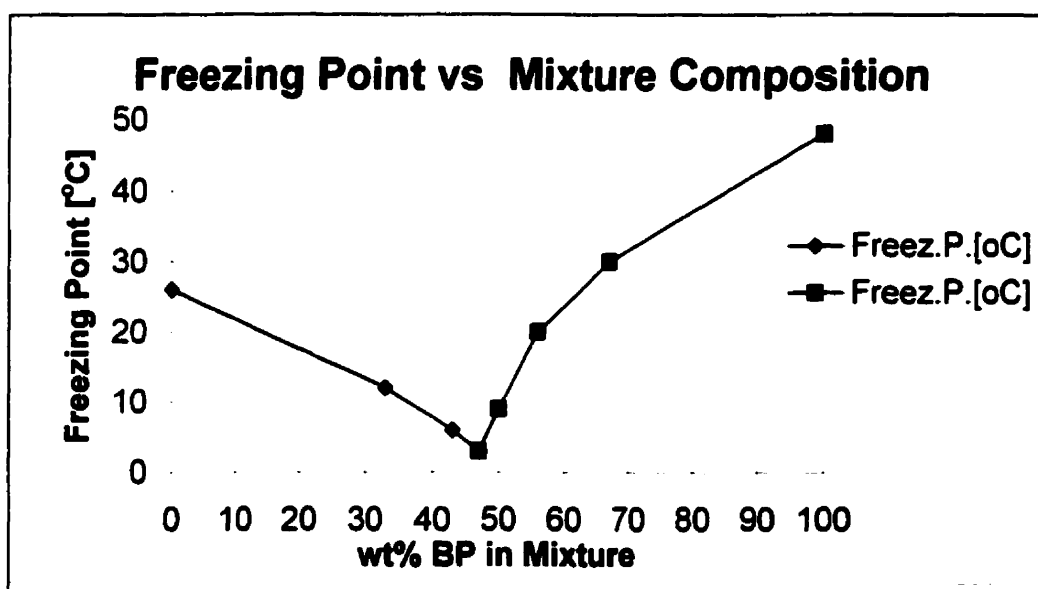


Figure 4.1: Phase Equilibrium Diagram of BP-TAC mixture

4.2 Additive Profiles

4.2.1 Radial Profile

Radial, concentration profiles of 5 mm diameter extrudate rods were obtained using micro FTIR analysis to monitor quantitatively the additives distribution across the polymer cross-section. The values of the concentrations were plotted versus extrudate diameter, where +2.5 and -2.5 represent opposite sides of the polymer surface (ends of the extrudate cross-section) with 0 as the centre (see Tables 4.2 and 4.3). Substantial concentration gradients have been observed only in the area close to the surface (around 0.5 mm from the surface). This is an indication that the evaporation did not extend very deeply into the extrudate.

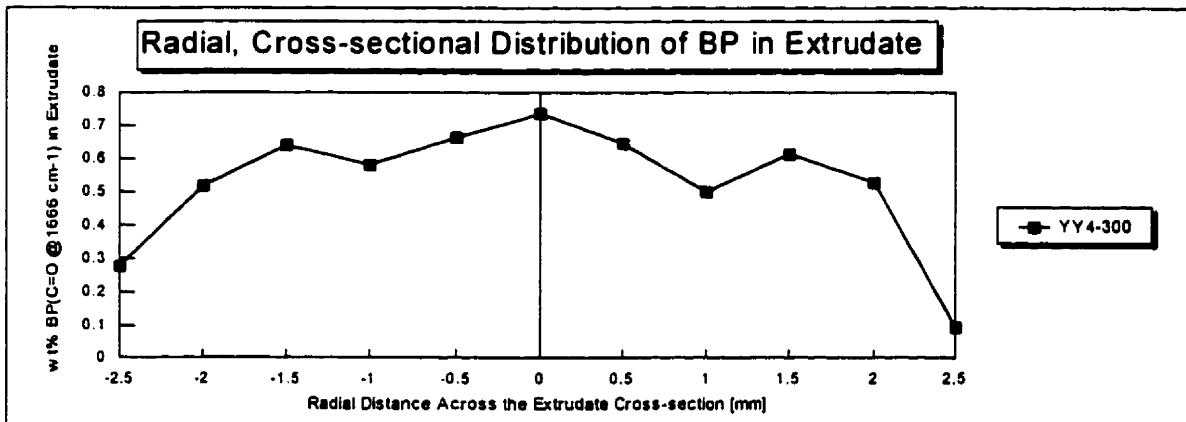


Figure 4.2: Concentration profile of BP across PE-extrudate cross-section.

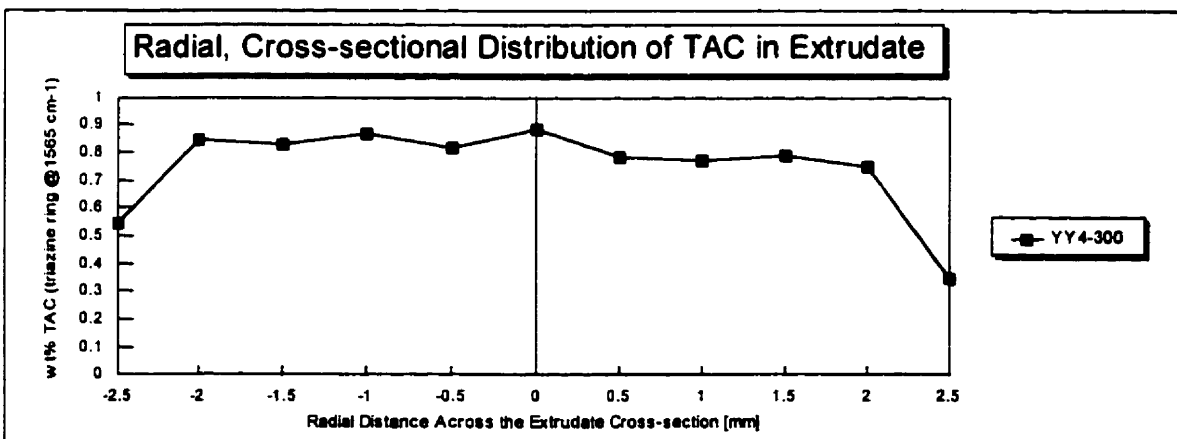


Figure 4.3: Concentration profile of TAC across PE-extrudate cross-section.

4.2.2 Axial Profile

Concentration profiles of 5 mm diameter extrudate rods were obtained using FTIR analysis to monitor quantitatively the additives distribution along the length of the polymer extrudate.

The values of the concentrations were plotted versus extrudate length (see Figures 4.4 through 4.7). Two sets of experiments were conducted, where the only variable was barrel temperature (set at 160 and 200°C respectively).

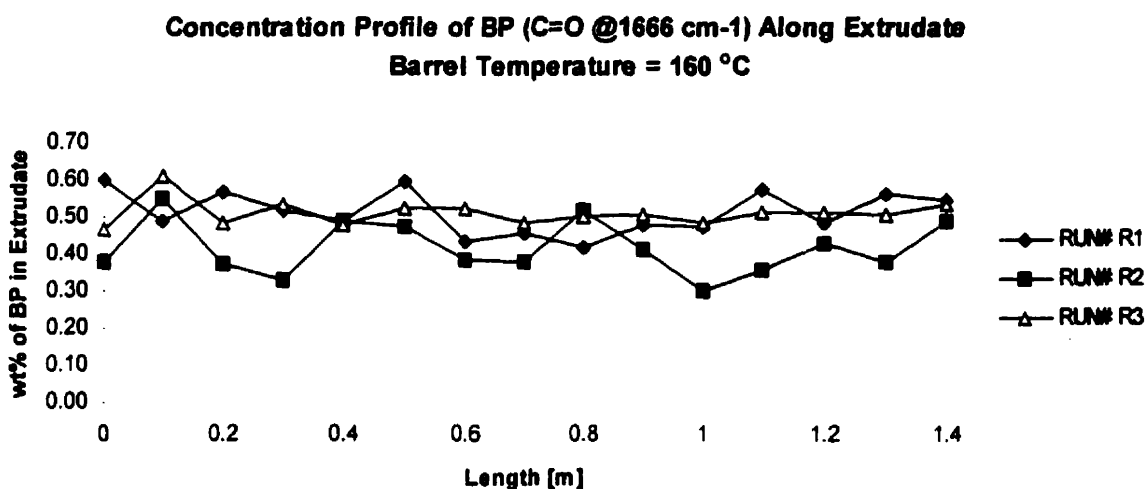


Figure 4.4: Concentration Profile of BP along Extrudate

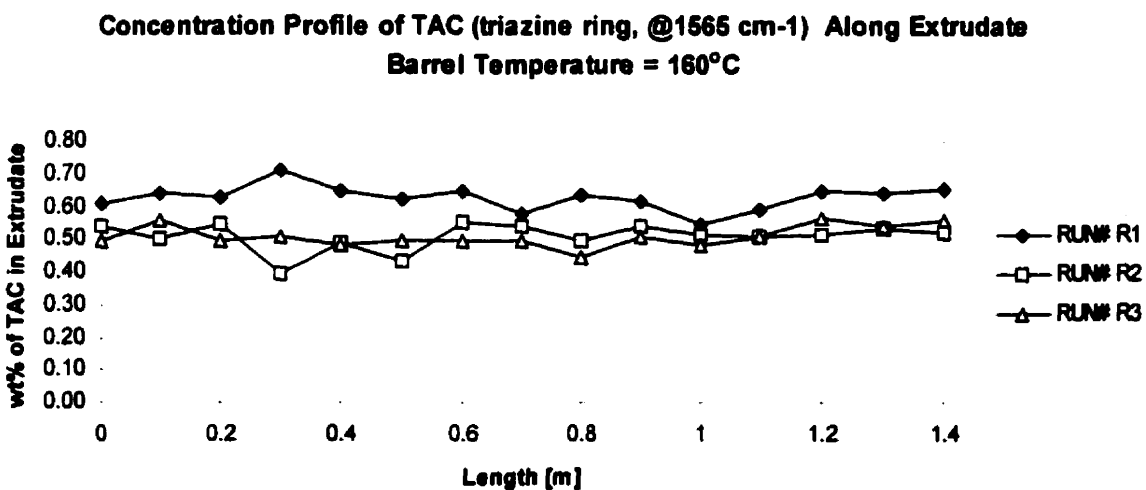


Figure 4.5: Concentration Profile of TAC along Extrudate

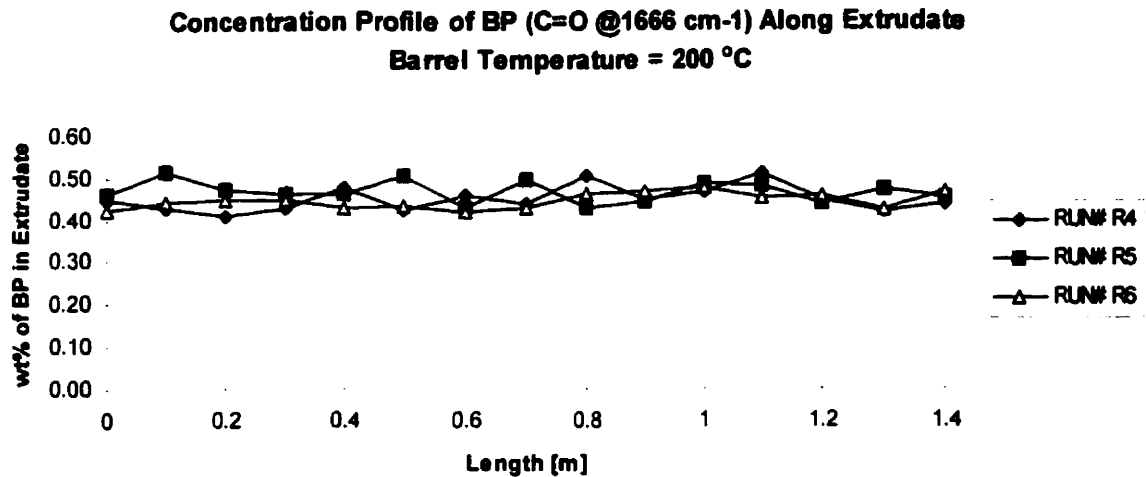


Figure 4.6: Concentration Profile of BP along Extrudate.

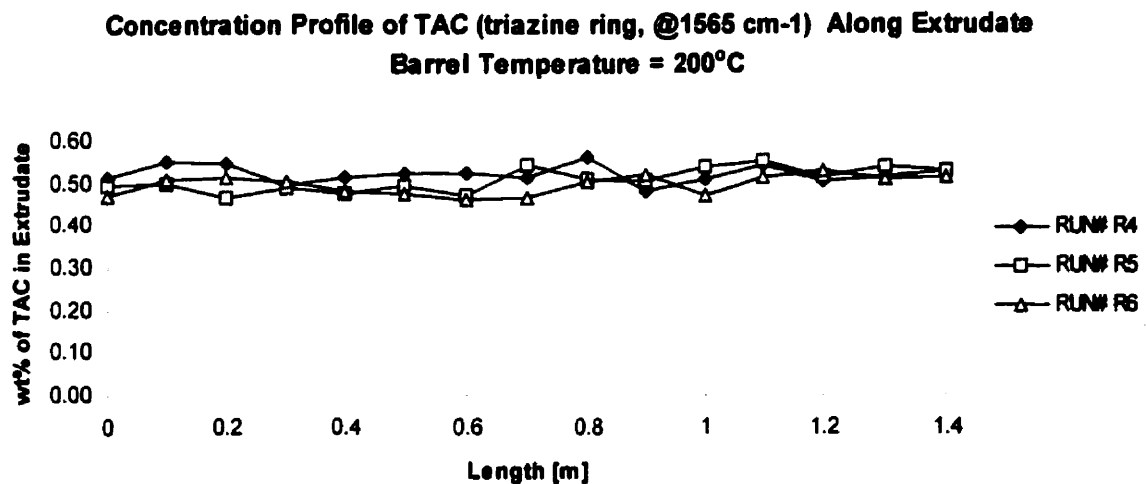


Figure 4.7: Concentration Profile of TAC along Extrudate

The standard deviation of BP and TAC concentrations at barrel temperatures 160 and 200°C were calculated and plotted on Figure 4.8 and Figure 4.9. The values of average additives concentration and their standard deviations were summarized in Table 4.2. The results obtained showed that the runs were carried out at steady state and the higher barrel temperature of 200°C promoted a uniform concentration distribution of both additives along the extrudate.

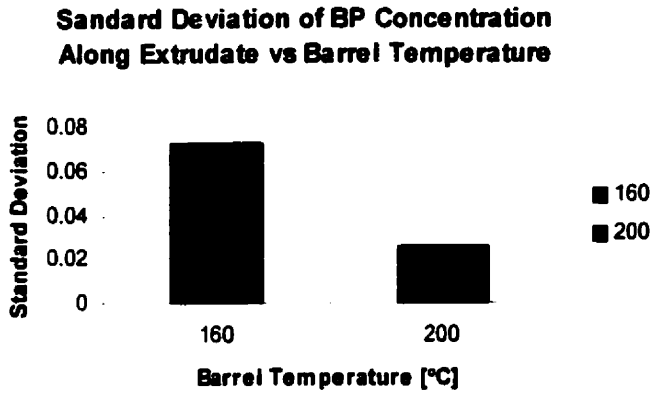


Figure 4.8: Standard Deviation of BP Concentration as a Function of Extruder Conditions.

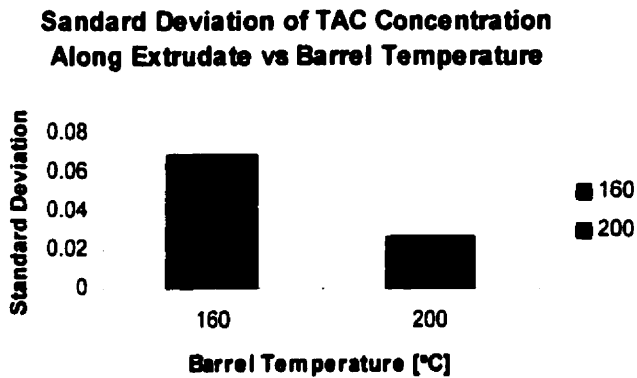


Figure 4.9: Standard Deviation of TAC Concentration as a Function of Extruder Conditions.

Barrel Temperature [°C]	Average BP Concentration in Extrudate [wt%]	Standard Deviation of BP Concentration in Extrudate	Average TAC Concentration in Extrudate [wt%]	Standard Deviation of TAC Concentration in Extrudate
160	0.48	0.0722	0.55	0.0687
200	0.45	0.0261	0.51	0.0261

Table 4.2: Additives Distribution along the Extrudate.

4.3 Effect of Processing Variables

4.3.1 Extrusion Conditions

Table 4.3 shows the results of the statistical 2^3 experimental design conducted on $4 \text{ mm} \pm 0.3 \text{ mm}$, FINA 7208, polyethylene extrudate rods with the objective determining the significance of extrusion variables (barrel temperature, die temperature and residence time. The response variable was percent additive loss. Controlled extrusion conditions experiments were conducted with input additives concentration constant $0.60 \pm 0.06 \text{ wt\%}$.

Run #	FACTOR			Additives Loss [wt%]	
	A Barrel Temperature [°C]	B Die Temperature [°C]	C Residence Time [min]	Benzophenone	TAC
1	160	160	25	20.32	2.24
2	160	160	6.25	21.46	5.64
3	160	190	25	17.83	4.34
4	160	190	6.25	5.99	8.16
5	200	160	25	18.41	5.17
6	200	160	6.25	9.06	7.72
7	200	190	25	13.75	6.15
8	200	190	46.25	15.94	5.39

Table 4.3: Statistical Analysis of Factorial Design.

In order to determine the effects of the extrusion variables on the loss of each additive two analysis-of-variance tables were generated, one for BP and one for TAC (see Tables 4.4 and 4.5). According to the results none of the variables investigated (barrel temperature, die temperature and extruder residence time) was a significant factor for the additives loss.

Source of variation (Factor)	Sum of squares (SS)	Degrees of freedom (DF)	Mean square MS (SS/DF)	Mean-Square ratio MSR (MS/MS _{residual})	F(0.05,1,4)
Residence time (A)	39.87245	1	39.87245	1.247149	7.71
Barrel temperature (B)	8.9042	1	8.9042	0.27851	7.71
Die temperature (C)	30.96845	1	30.96845	0.968646	7.71
AB interaction	1.56645	1			
AC interaction	0.2592	1			
BC interaction	50.90405	1			
ABC interaction	75.1538	1			
Residual (error) term	127.8835	4	31.97088		

Table 4.4: Analysis of Variance Table for Loss of Benzophenone

Source of variation (Factor)	Sum of squares (SS)	Degrees of freedom (DF)	Mean square MS (SS/DF)	Mean-Square ratio MSR (MS/MS _{residual})	F(0.05,1,4)
Residence time (A)	10.14751	1	10.14751	3.715728	7.71
Barrel temperature (B)	2.050313	1	2.050313	0.750766	7.71
Die temperature (C)	1.336613	1	1.336613	0.489429	7.71
AB interaction	3.685613	1			
AC interaction	1.044013	1			
BC interaction	4.455113	1			
ABC interaction	1.739113	1			
Residual (error) term	10.92385	4	2.730963		

Table 4.5: Analysis of Variance Table for Loss of TAC

4.3.2 Input Additive Concentration

In order to determine the sources of additive loss and to optimize the process of additives incorporation, a set of experiments were conducted where the extrusion conditions were kept constant (same as Run #4 of the three factorial statistical experimental design) and the input concentration of additives was varied in wide range from 0.54 to 2.8 wt% of each additive.

For the extruder conditions used a combination of the lowest barrel temperature with the highest possible screw speed (RPM = 10) has been selected (see Table 4.3).

The results for the additives incorporation using this particular twin-screw extruder are shown on Figures 4.10 through 4.13. According to these results the output concentration of BP and TAC in extrudate and the losses of both additives strongly depended on input additive concentration. All of these dependencies could be well expressed by a second degree polynomial. The targeted 1 wt% of each additive incorporated into the polymer was not reached. The results summarized in Table 4.4 showed that the losses of both BP and TAC were approximately equal under the same conditions. They became substantial at input concentrations exceeding 1 wt%. This was attributed to insufficient mixing in the extruder of the low viscosity additive mixture. The maximum amounts of additives incorporated were 0.79 wt% for BP and 0.84 wt% for TAC.

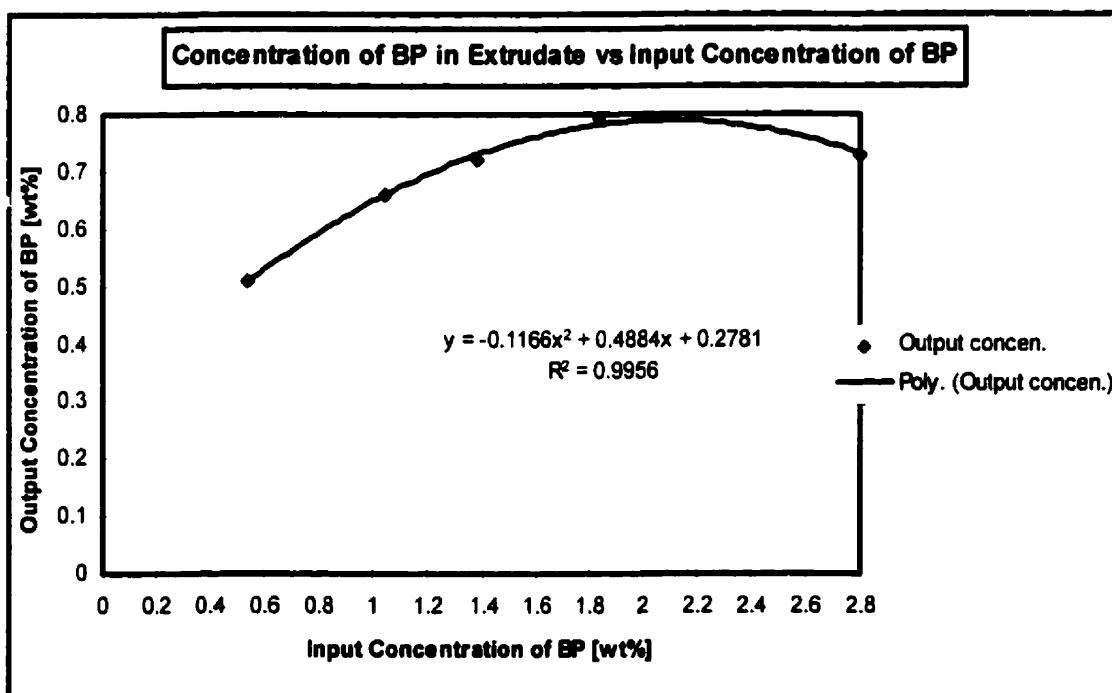


Figure 4.10 : Output Concentration of BP as a Function of Input Additive Concentration

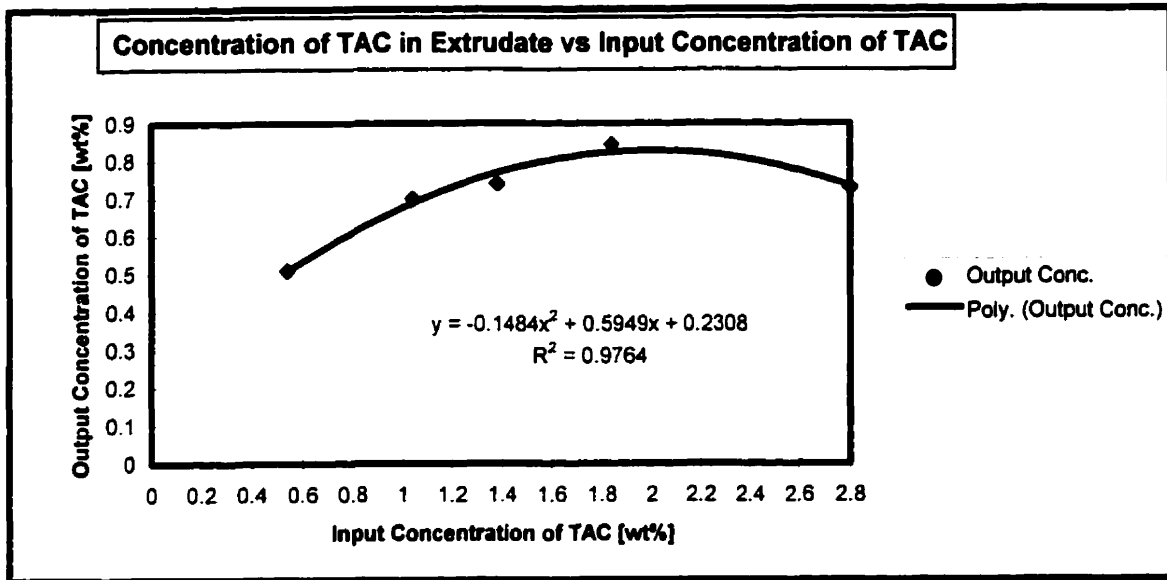


Figure 4.11: Output Concentration of TAC as a Function of Input Additive Concentration

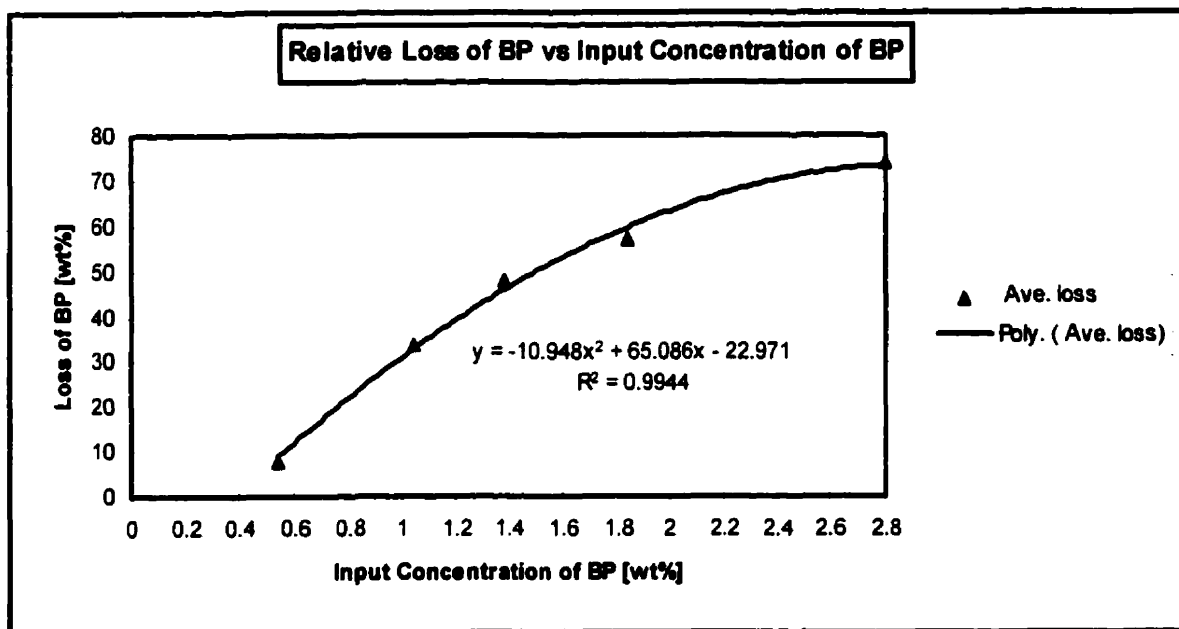


Figure 4.12 : Loss of BP as a Function of Input Additive Concentration

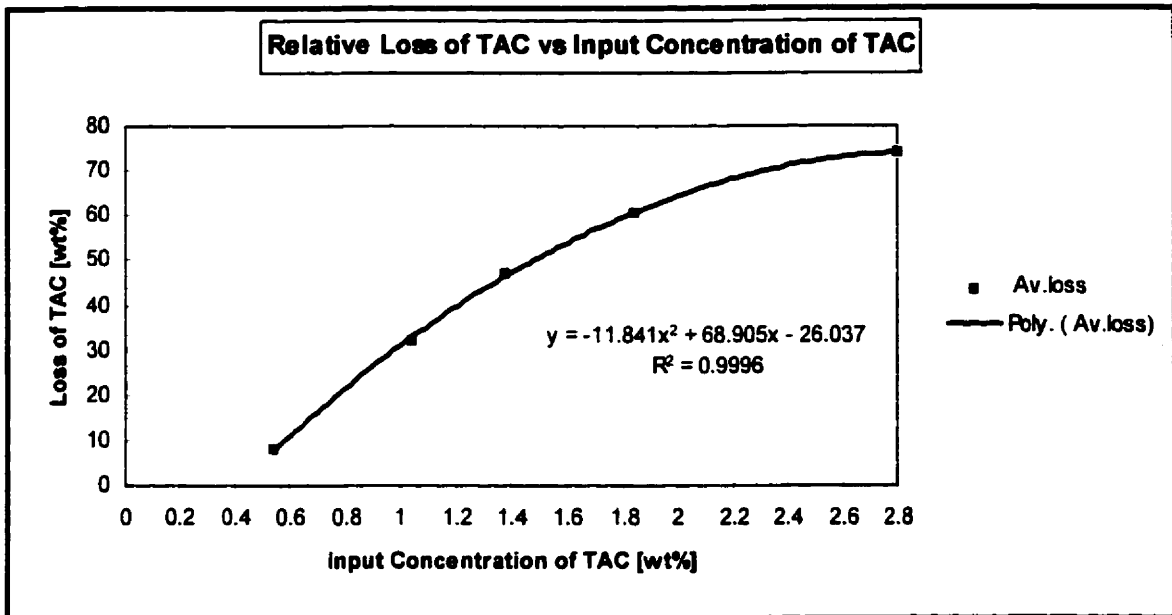


Figure 4.13: Loss of TAC as a Function of Input Additive Concentration

In an attempt to collect more evidence about the mechanism of the additive loss , an additional experiment was conducted at high input concentration of 1.84 wt% for each additive. After five hours running the extruder was disassembled and the inside of the barrel was inspected. A liquid additive mixture was found deposited on the wall of the barrel in the low pressure zone.

4.4 Two Stage Incorporation

The results of the previous section led to the idea of using a two stage process to obtain higher final additive concentrations. The addition of two low concentrations of additives in two separate runs could each exploit the higher efficiencies (lower losses) at the low additive concentrations. Their sum would together then provide higher concentrations than previously obtained. The same counterrotating twin-screw extruder was used. The extruder settings (same as run #4 of three-factorial statistical experimental design) were maintained constant and an input total (BP + TAC) additive concentration of 2.8 wt% was maintained during a two stage incorporation process. The extrudate produced with the first stage was pelletized and consequently fed into extruder for the second stage of the additive

incorporation. The results summarized in Fig.4.5 and 4.6 showed that steady state concentrations of 1.33 wt% for BP and 1.46 wt% for TAC were obtained at the two stages addition. The results also showed that concentrations of 0.67 wt% BP and 0.73 wt% TAC were incorporated in each of the two stages. This is in agreement with the improved efficiencies at low concentrations shown in Figures 4.10 and 4.11.

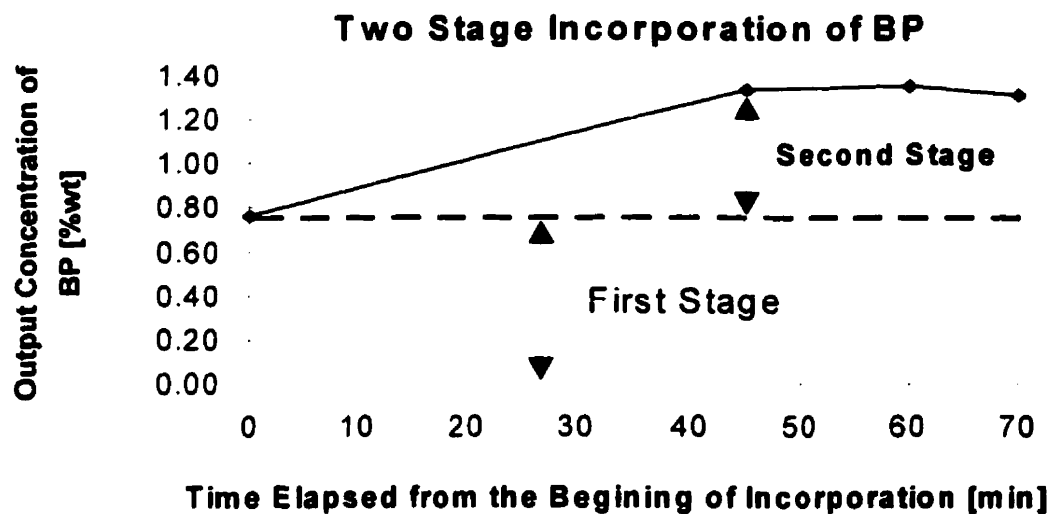


Figure 4.14: %wt. BP Incorporated during the Two Stage Incorporation Process

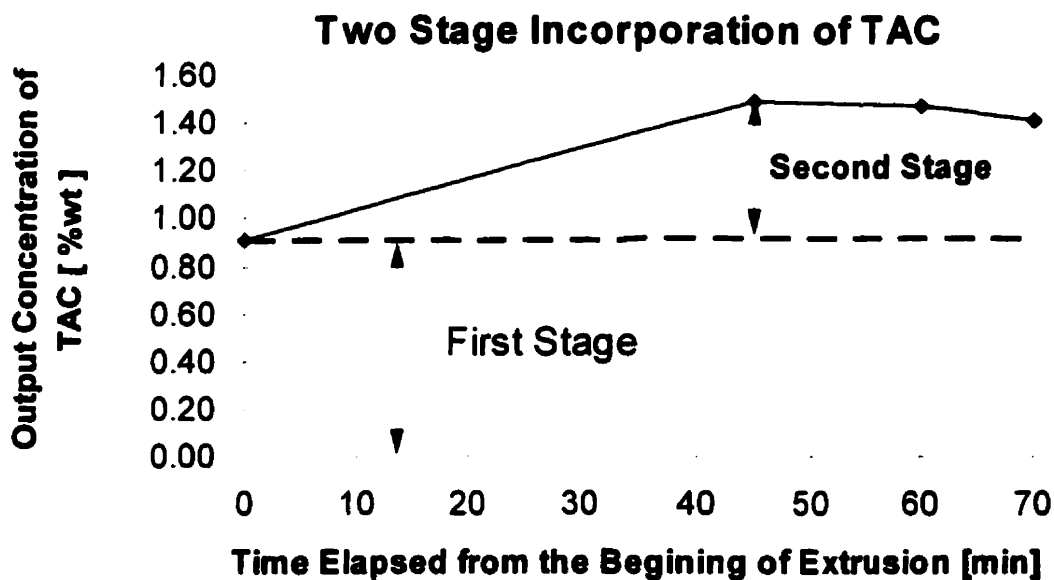


Figure 4.15: %wt. TAC Incorporated during the Two Stage Incorporation Process

4.5 Extruder Residence Time Distributions

Two sets of experiments were conducted using pulse stimulus-response technique and a tracer already described in section 3.5. The theoretical details are given in section 2.4. The only variable was barrel temperature (set at 160 and 200^oC respectively). The other extruder conditions were maintained constant and they were summarized in Table 3.6. The amount of pulse injection was 0.16 g of the tracer system.

Concentrations of the tracer in extrudate as function of time elapsed after pulse injection were obtained for every component of the tracer system. They were plotted on Figures 4.16, 4.19, and 4.22. Based on this data, the residence-time distribution functions were calculated (Equations 3 and 5) and plotted on Figure 4. 17, 4.20, and 4.23. The mean residence times were calculated (Equation 7) and shown on Figures 4.18, 4.21, and 4.24.

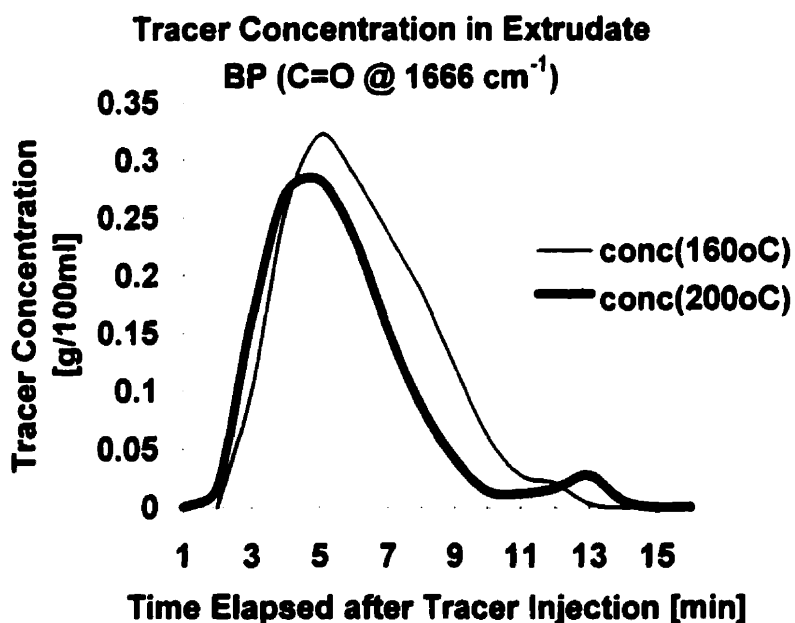


Figure 4.16: Tracer Concentration (BP) in Extrudate versus Time

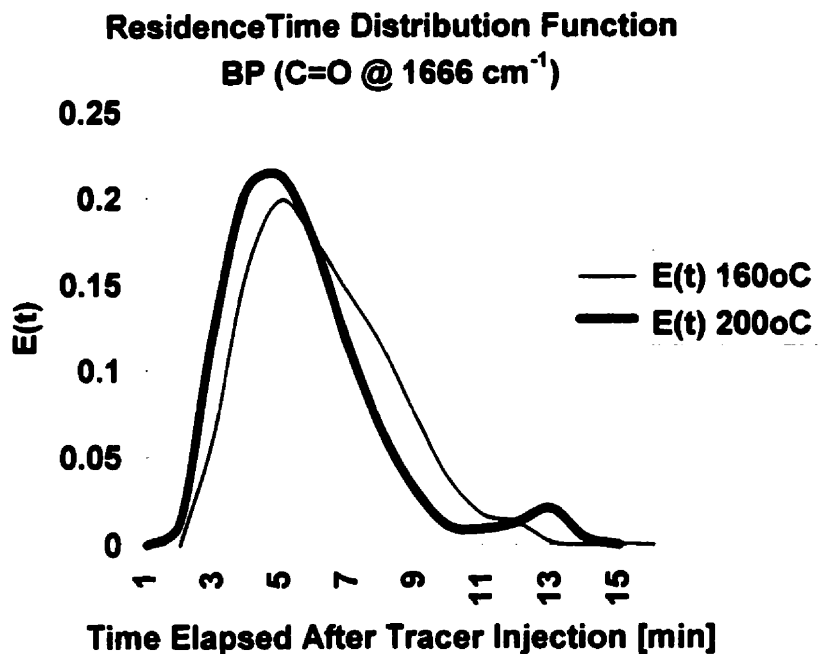


Figure 4.17: Residence Time Distribution Function as a Function of Extruder Conditions.

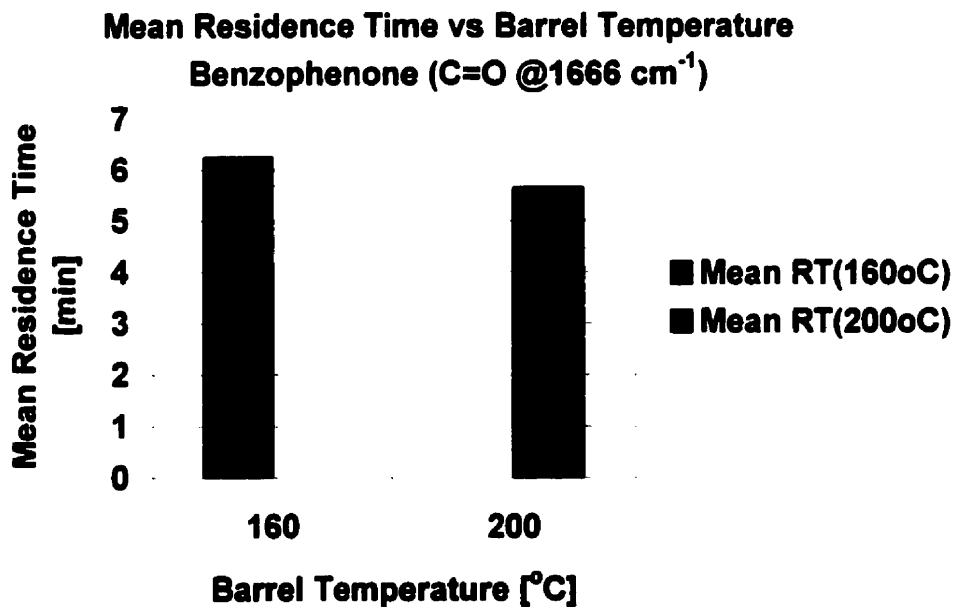


Figure 4.18: Mean Residence Time as a Function of Barrel Temperature

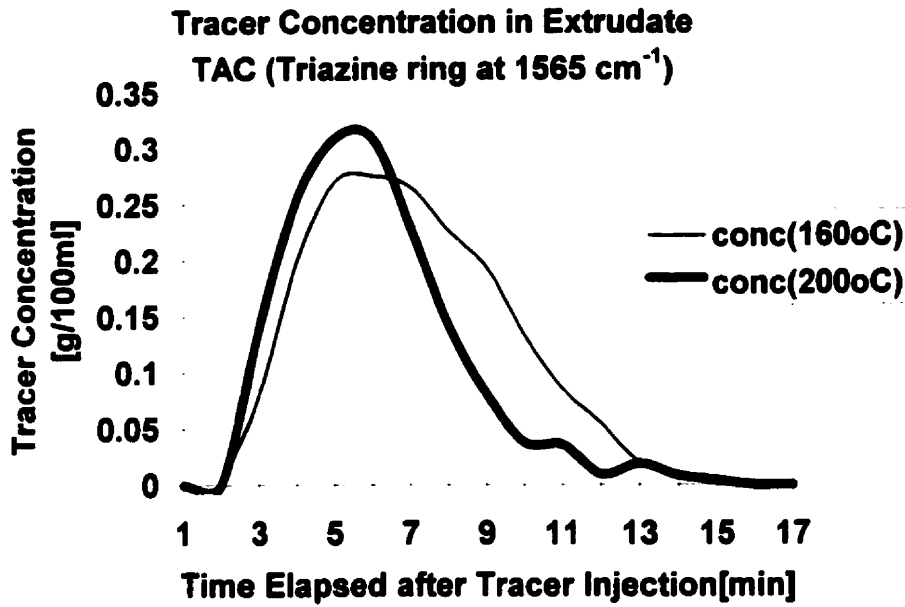


Figure 4.19: Tracer Concentration (TAC) in Extrudate versus Time

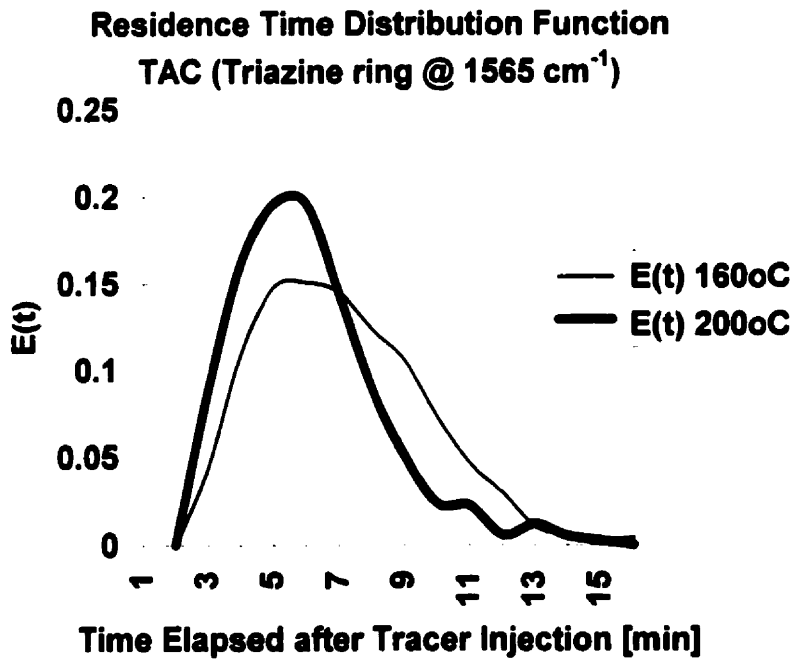


Figure 4.20: Residence Time Distribution Function as a Function of Extruder Conditions.

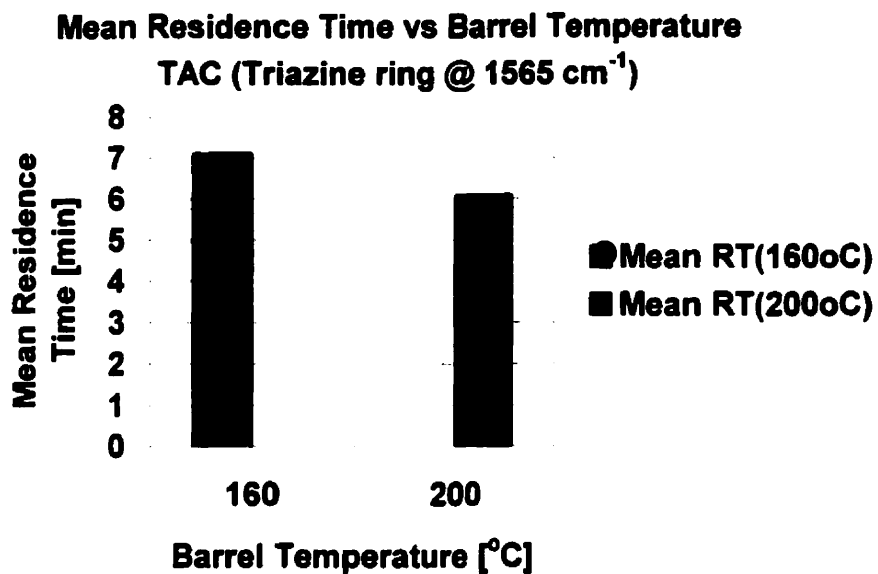


Figure 4.21: Mean Residence Time as a Function of Barrel Temperature

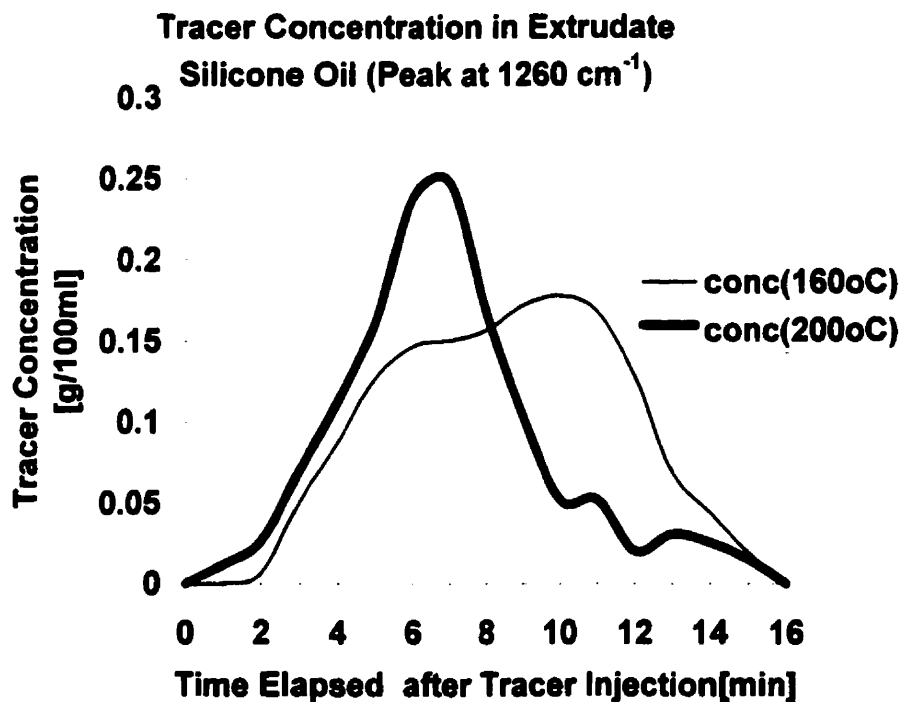


Figure 4.22: Residence Time Distribution Function as a Function of Extruder Conditions.

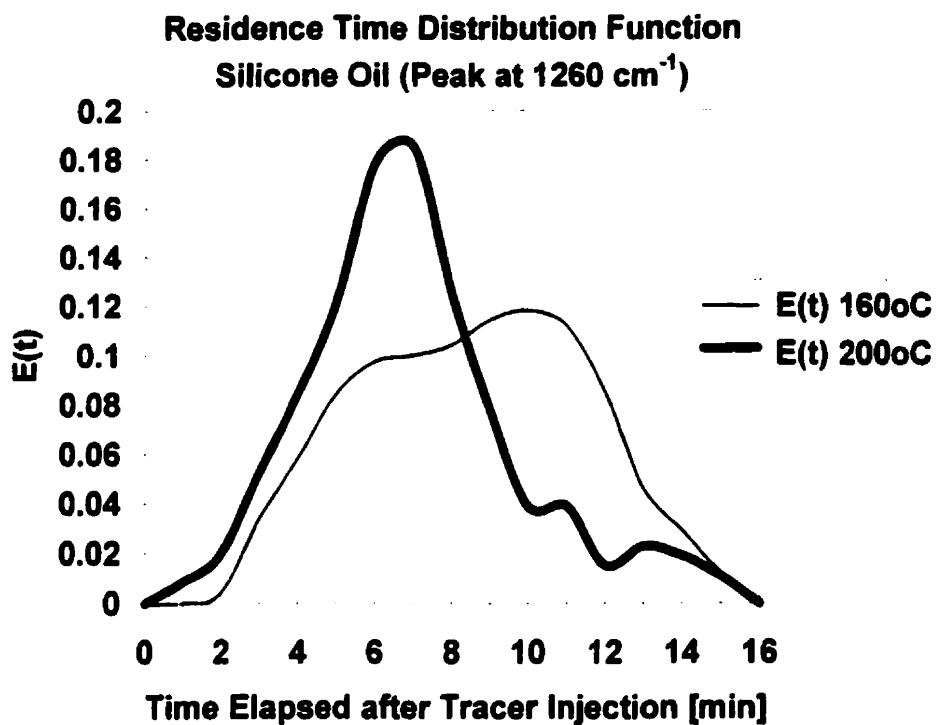


Figure 4.23: Residence Time Distribution Function as a Function of Extruder Conditions.

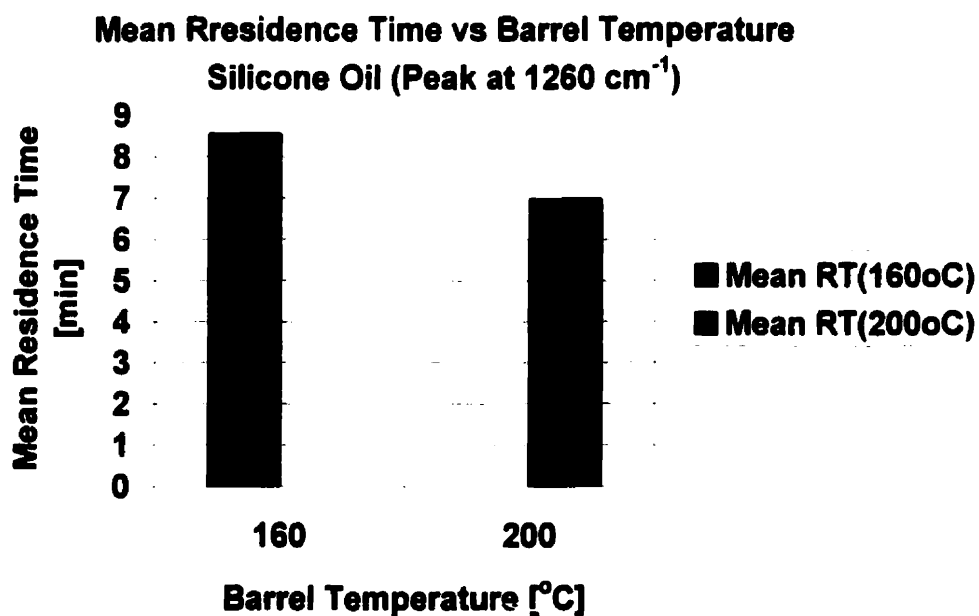


Figure 4.24: Mean Residence Time as a Function of Barrel Temperature

In order to determine whether or not there was extruder “deadvolume” region, the normalized times (θ) were calculated (Equation 2) and area beyond the cutoff point at $\theta = 2$ were examined. The tail area under the curve of the residence time distribution function (extruder “deadvolume” fraction) was numerically integrated using the Trapezoidal Rule. The results were summarized in Table 4.6.

	Barrel Temperature 160°C	Barrel Temperature 200°C
Mean Residence Time (BP) [min]	6.24	5.64
Mean Residence Time (TAC)[min]	7.11	6.02
Mean Residence Time (Silicone Oil) [min]	8.54	6.95
Extruder Deadvolume Fraction (BP)	0.02	0.05
Extruder Deadvolume Fraction (TAC)	0.02	0.04
Extruder Deadvolume Fraction (Sil. Oil)	0.01	0.04

Table 4.6 : Mean Residence Time and Extruder Deadvolume Fraction.

The analysis of Table 4.6 showed that there was no extruder deadvolume regions since the extruder deadvolume fraction in all cases was negligible. However, this type of analysis uses a normalized (unit area) curve. Thus dead volume which completely retains a portion of the tracer (without leaving a long tail on the distribution) is not visible.

4.6 Additional Evaluation of Effect of Temperature by Use of Three-Components Additive Mixture

An experiment with the three-components liquid additive mixture (BP, TAC, silicone oil) was conducted in order to compare the loss of BP and TAC with the loss a high temperature resistant component (silicone oil). The three-component mixture contained BP, TAC and high-temperature resistant (up to 240°C) silicone oil in equal weight amount. The results were shown on Figures 4.24 and 4.25. The extruder condition profile was: barrel temperature = 200°C, die temperature = 190 °C and screw speed = 10 RPM.

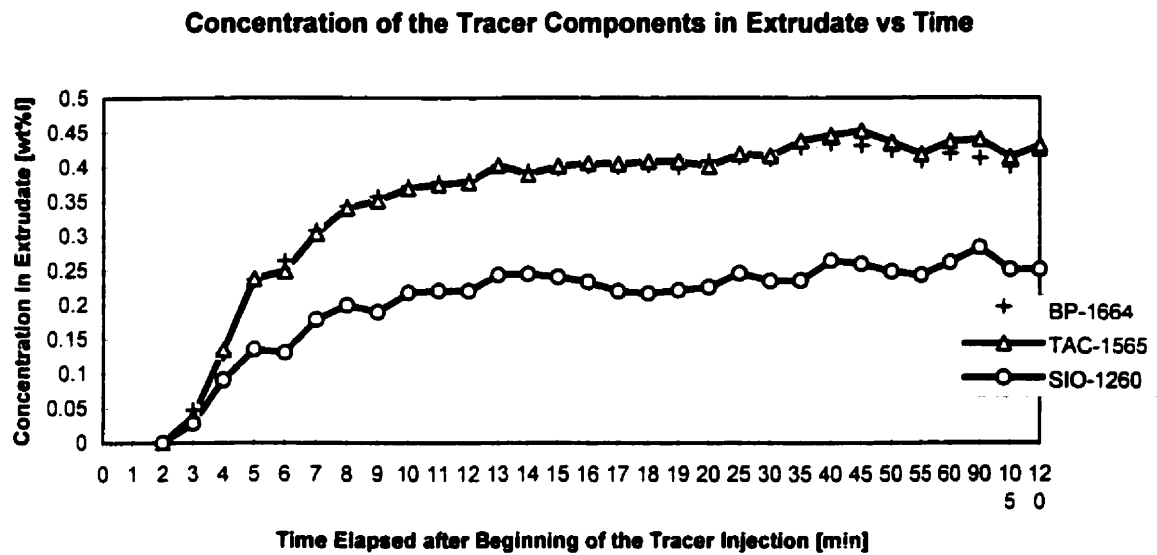


Figure 4.25: Concentration of the Tracer Components versus Time

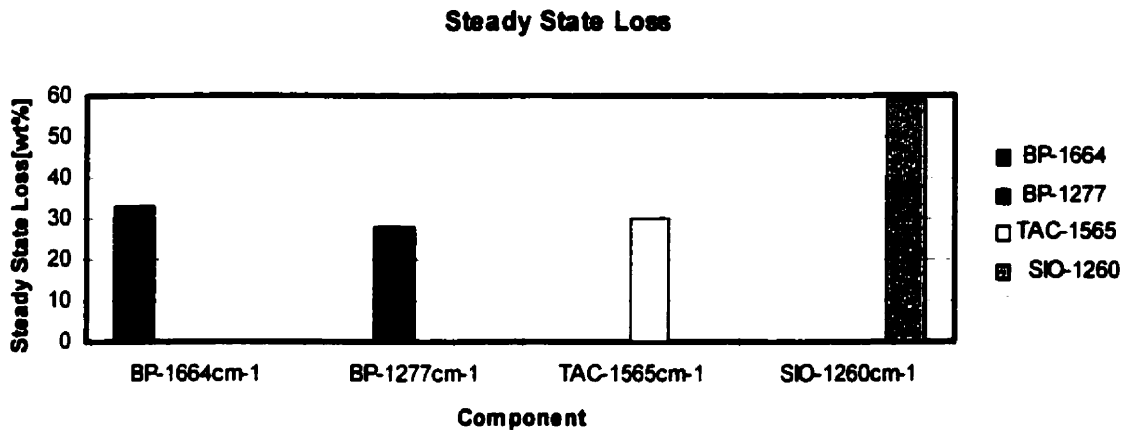


Figure 4.26: Loss of Tracer Components at Steady State Extruder Condition

The results showed that the loss of silicone oil (silicone oil in Figures 4.24 and 4.25) (59%) is twice as high as the loss of BP (31%) and TAC (30%). This cannot be explained by evaporation due to high processing temperature.

4.7 Additive Incorporation with High Intensity Internal Batch Mixer

Experiments with a high intensity internal batch mixer were conducted with two objectives:

- to obtain concentrates of BP and TAC in HDPE;
- to investigate the effect of the processing temperature on additives loss.

The equipment and experimental procedure were described in the previous sections 3.2.2 and 3.3.4. The results obtained are given in Table 4.6 and Table 4.7.

Batch #	Processing Temperature [°C]	Mass of Pellets [g]	Mass of Additives Added [g]	Mass of Final Specimen [g]	Mass of Additives Incorpor. ⁽¹⁾ [g]	Total % Additives Incorpor. ⁽²⁾ [wt%]	Total Additives Loss ⁽³⁾ [wt%]
1	170	41.2	33.3	68.9	27.7	40.2	13.81
2	170	41.2	26.7	65.0	23.8	36.61	10.86
3	170	41.2	28.2	67.3	26.1	38.78	7.44
4	190	41.2	30.8	69.4	28.2	40.63	8.44
5	190	41.2	30.8	68.3	27.1	39.68	12.01
6	190	41.2	29.6	66.6	25.4	38.14	14.19

Table 4.7 Processing Conditions and Results of Additive Incorporation with the High-Intensity Internal Batch Mixer.

⁽¹⁾ = Mass of final specimen - Mass of pellets

⁽²⁾ = (Mass of additive incorporated / Mass of final specimen)*100

⁽³⁾ = 100*(Mass of additives added - Mass of additives incorporated)/Mass of additives added

Processing Temperature [°C]	Average Total Additives Concentration [wt%]	Average Total Additives Loss [wt%]
170	38.53	10.70
190	39.48	11.55

Table 4.8 Average Total Additives Loss and Average Total %wt. Additives Incorporated with the High-Intensity Internal Batch Mixer.

The results showed that a very high percentage of investigated additives can be incorporated into HDPE. The additive loss during the incorporation process is relatively small (10 to 12 wt%) and not influenced by the processing temperature. This provided additional evidence that processing temperature was not a significant factor for the additive loss.

5.0 CONCLUSIONS

Conclusions:

- The additives BP and TAC form a mobile liquid as a 50:50 mixture by weight and can be metered into the polymer orientation process.
- An FTIR method capable of determining both average concentration profile across the cross-section of the extruded strands was developed for both BP and TAC.
- Additive losses for the equipment used here originated mainly from accumulation on the wall of the extruder.
- Extruder temperature and rpm had no significant effect on additive loss. Evaporation of additive was not a major source of additive loss in this system for the range of operating conditions examined.
- Residence time distribution experiments conducted using BP, TAC and silicone oil (a non-volatile tracer) demonstrated high losses for the latter and provided additional evidence that evaporation was not a significant factor for additive losses.
- Using a two stage process, additive losses were minimized so that high concentrations (1.3 wt% BP and 1.5 wt. % TAC) could be incorporated into the product.

6.0 NOMENCLATURE

Δ	change
λ	wavelength (nm)
ρ	density (g/ml)
A	absorbance
b	path length (cm)
BP	benzophenone
c	concentration
C-C•H ₂	alkyl radical
cm	centimeter
e	exponential
FTIR	Fourier transform infrared
h	Plank's constant
I	intensity
In	photoinitiator
IR	infrared
M _n	number average molecular weight
M _w	weight average molecular weight
nm	nanometer (10⁻⁹)
P•	alkyl radical on PE chain
P•'	allyl radical on PE chain
PE	polyethylene
(PI)*	excited state of photoinitiator
PT•	intermediate radical formed by P and T•
PT	intermediate formed by P•' and T•
PT• _n	propagating radical of polyethylene molecule and TAC allyl radical
T•	TAC allyl radical
TAC	Triallyl Cyanurate
R•	alkyl radical
R'H	polyolefin molecule
t	time(min)
T1	electronic triplet state
UV	ultraviolet radiation
wt	weight

7.0 REFERENCES

1. A. Charlesby and S.H. Pinner, Proc. R.Soc. London Ser. A, 249, 367 (1959).
2. A. Charlesby, C. S. Grace, and F. B. Pilkington, Proc. R. Soc. London Ser. A, 268, 205 (1962).
3. de Boer, J.; Pennings, A.J. Makromol. Chem., Rapid Commun, 1981, 2, 749.
4. de Boer, J.; Pennings, A.J. Polymer 1982, 23, 1944.
5. R. Howath, Elektroizolachna Kablova Tech., 39,14 (1986); cf. Chem. Abstr., 106, 106, 68188 (1987).
6. G. Oster, J. Polymer.Sci.,22,185 (1956).
7. G. Oster, G.K.Oster, and H.Moroson, J. Polym Sci., 34, 671 (1959).
8. H. Wilski, Angew. Chemm., 71, 612 (1959).
9. Chien, P. C. Chiang and E. C. Hou, Collected Papers of the Institute of Applied Chemistry (China), 4, 145 (1960); Vysokomol. Soedin., 1, 635 (1959).
10. R. M. Ikeda, B. R. Gelin, F.F. Rogers and S. Tocker, Coat. Plast. Prepr., 35(1), April 90 (1975).
11. B. Ranby and P. Carstenaen, Adv. Chem. Ser., 66, 256 (1967).
12. V.K. Milinchuk and S.Ya. Pahezhtskii, Vysokomol. Soedin., 5, 946 (1963).
13. S. Ohnishi, S. Sugimoto, and I. Nitta, J. Chem. Phys., 39, 2647 (1963).
14. Labana, S.S. (ed) Ultraviolet Light Induced Reactions in Polymers, ACS Symp. Ser. 1976, Vol. 25.
15. J. Hillborn and B. Ranby, Macromol. 22 1154 (1989).
16. P. V. Zamotaev, N. I. Litsov, and A. A. Kachan, Vysokomol. Soedin., B24(8), 577 (1962).
17. P. V. Zamotaev, V. M. Granchak, N. I. Litsov and A. A. Kachan, Vysokomol. Soedin., A27(10), 2072 (1985).
18. Zamotaev P.V., N. I. Litsov, and A. A. Kachan, Vysokomol. Soedin., Polym. Photochem., 7(2), 139 (1986).
19. Zamotaev P.V. and Mityukhin O.P., Photochemical Cross-linking Linear Polyethylene, Ukrainskii Khimicheskii Zhurnal, 58, 811 (1992).

20. Z.O. Streltsova, L.A. Negievich and A. A. Kachan, Dopov. Akad. Nauk, Vkr. Rer. B: Geol. Khim. Biol. Nauki, (5), 75 (1982).
21. L.P. Klimenko, L.A. Negievich, and A. A. Kachan, Vysokomol. Soedin., B 24(11), 834 (1982).
22. Yan Qing and Bengt Ranby, Photoinitiated Crosslinking of Low Density Polyethylene, J. Polymer Eng. Sci. , 32, 831 (1992) (part IV of the series).
23. Yan Qing and Bengt Ranby, Photoinitiated Crosslinking of Low Density Polyethylene, J. Polymer Eng. Sci. , 32, 1433 (1992) (part V of the series).
24. Yong Lie Chen and Bengt Ranby, Photocrosslinking of Polyethylene, J. Polymer Sci., 27, 4051 (1989) (part I of the series).
25. Yong Lie Chen and Bengt Ranby, Photocrosslinking of Polyethylene, J. Polymer Sci., 27, 4077 (1989) (part II of the series).
26. Yong Lie Chen and Bengt Ranby, Photocrosslinking of Polyethylene, J. Polymer Sci., 28, 1847 (1990) (part III of the series).
27. Ranby, "Photoinitiated Reactions of Organic Polymers", in Polymer Science in the Next Decade, International Symposium Honoring Herman F.Mark on his 90th Birthday, May 1985, O. Volg and E.H. Immergut, Eds. Wiley, New York 1987, pp. 121-133.
28. B. Ranby, "Photoinitiated Crosslinking of Polymers", presented at IUPAC International Symposium on Polymers for Advanced Technologies, Jerusalem, Israel, Aug. 16-21, 1987, VCH Publ., New York, 1988, pp. 162-181.
29. Yan Qing, Xu Wenying, and Bengt Ranby, Photoinitiated Crosslinking of Low Density Polyethylene, J. Polymer Eng. Sci. , 31, 1561 (1991) (part I of the series).
30. Yan Qing, Xu Wenying, and Bengt Ranby, Photoinitiated Crosslinking of Low Density Polyethylene, J. Polymer Eng. Sci. , 31, 1567 (1991) (part II of the series).
31. Suanda, S. Patent #9314344.4. "Continuous Process for the Manufacture of Crosslinked, Oriented Polyethylene Extrudates".
32. Charles E. Hoyle, and J.F. Kinstle. "Radiation Curing of Polymeric Materials". American Chemical Society , Washington D.C. (1990). Pp. 1-41.
33. Zamotaev, Pavel, and Chodak, Ivan. "Photocrosslinking of Oriented Ultra-High Molecular Weigh Polyethylene". Die Angewandie Makromolekulare Chemie 210

- (1993). Pp.119-128.
34. Friedhelm Hensen, *Plastics Extrusion Technology*, 1988, p.25, 26,32, 41, 43, 307, 309, 317,322, 323, 325, 326, 435, 436, 489, 490, 491, 507.
 35. R. Gachter and H. Muller, *Plastics Additives*, 1985, p.658, 715, 729-741,
 36. Rauwendaal Chris, *Mixing in Polymer Processing*, Dekker, 1991.
 37. Lutz J.T., *Thermoplastic Polymer Additives*, Dekker, 1989.
 38. Kresta Jiri E., *Polymer Additives*, Plenum Press, 1984.
 39. Findlay, Alexander. *The Phase Rule and Its Applications*, New York Longmans, Green 1927.
 40. Crompton T.R., *Chemical Analysis of Additives in Plastics*, 1971, p.1, 2,
 41. Miller, R.G.J. and Willis, H.A., *Spectrochim. Acta* 14, 119(1959)
 42. Luongo, J. P., *Applied Spectroscopy* 19, (4), 117 (1965).
 43. Drushel, H.V. and Sommers, A.L., *Anal.Chem.*36, 836 (1964).
 44. Bruno M. Fanconi, *Journal of Testing and Evaluation*, JTEVA, Vol. 12, (1), 33-39, (1984).
 45. Griffiths, P.R., "Forty Years of FT-IR Spectrometry". *Ana. Chem.*, 64 (18), 868-875, (1992).
 46. Griffiths, P.R., *Chemical Infrared Fourier Transform Spectroscopy* (New York: JohnWiley & Sons), 1975.
 47. Hobart H. Willard, L.L, Merrit, Jr. and John A. Dean. *Instrumental methods of Chemical Analysis*, D.Van Nostard Company, New York,1974.
 48. John R. Ferrarao and Louis J. Basline, Eds. *Fourier Transform Infra-red Spectroscopy*, Vol. I & II, Academic Press, 1978.
 49. Mattson Product Literature.
 50. McGraw-Hill Encyclopaedia of Chemistry, editor Parker, S.P., McGraw-Hill Book Company, (1983).
 51. S.L. Murov, *Handbook of Photochemistry*, Dekker, New York, 1973, p. 119.
 52. G. Socrates, *Infrared Characteristic Group Frequencies*, Willey, New York, 1980, p.96.
 53. Noble, D., "FT-IR Spectroscopy: It's all done with mirrors". *Analytical Chemistry*, June 1, 382-385, (1995).

54. Peter R., Griffiths and J. A., Haseth "Fourier Transform Infrared Spectrometry" 1986.
55. Svehila. G, Comprehensive Analytical Chemistry, Vol. VI, Analytical Infra-red Spectroscopy, Elsevier Scientific Publishing Company, 1976.
56. Danckwerts P.V., Appl. Sci. Res., A, 3, 279 (1952).
57. Danckwerts P.V., Chem. Eng. Sci., 2,1 (1953).
58. Levenspiel O., Chemical Reaction Engineering, Ch. 9, Wiley, New York, 1962.
59. Bigg D. & Middleman, Ind. & Eng. Chem. Fundamentals, 13, 1, 66 (1974).
60. Todd David B., Residence Time Distribution in Twin-Screw Extruders, J. Polymer Eng. & Sci. , 15, 437 (1975).
61. Janssen L.P.B.M., Twin Screw Extrusion, Elsevier, New York, 95 (1978).
62. Janssen L.P.B.M., Hollander R.W., Spoor M.W., and Smith John m., Residence Time Distributions in a Plasticating Twin Screw Extruder, J. Polymer Eng. & Sci. , 25, 345 (1979).
63. Rauwendaal C.J., Technical Papers, 38th Annual Technical Conference, SPE, 618 (1980).
64. Walk C.J., Technical Papers, 40th Annual Technical Conference, SPE, 423 (1982).
65. Wolf D. & White D.H., AIChE Journal, 22, 1 , 122 (1976).
66. Schott N. R. & Saleh D.V., Technical Papers, 36th Annual Technical Conference, SPE, 536 (1978).
67. Todd D.B. & Irving H.F., Chemical Engineering Progress, 65, 9, 84 (1969).
68. Werner H. & Eise K., Technical Papers, 37th Annual Technical Conference, SPE, 181 (1979).
69. Golba J.C., Jr., Technical Papers, 38th Annual Technical Conference, SPE, 83 (1980).
70. Nichols R.J., Golba J.C., and Shete P.K., AIChE Diamond Jubilee Meeting, Washington, D.C., October 31 - November 4, 1983.

APPENDIX I: Properties of Materials Used

APPENDIX I: Properties of Materials Used

Benzophenone

Mw = 182.22 g/mol

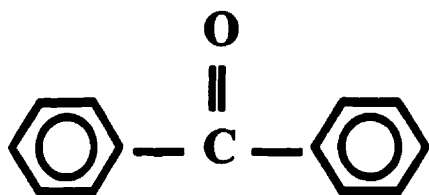
MP = α (48.1 °C); β (26 °C)

BP = 305.9 °C

ρ = α (1.146); β (1.1076) g/cc

η_D = α (1.6077); β (1.6059)

Soluble in: methanol, ethanol, benzene, xylene



2, 4, 6, Triallyloxy - 1, 3, 5, Triazine (Triallylcyanurate)

Mw = 249.27 g/mol

MP = 26 -28 °C

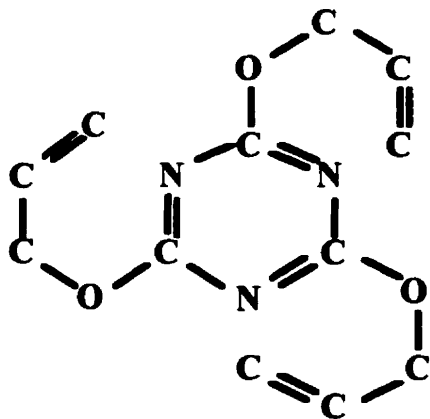
BP = 140 °C @ 0.5mm

ρ @ 30 °C = 1.1133 g/cc

η_D @ 25 °C = 1.5059

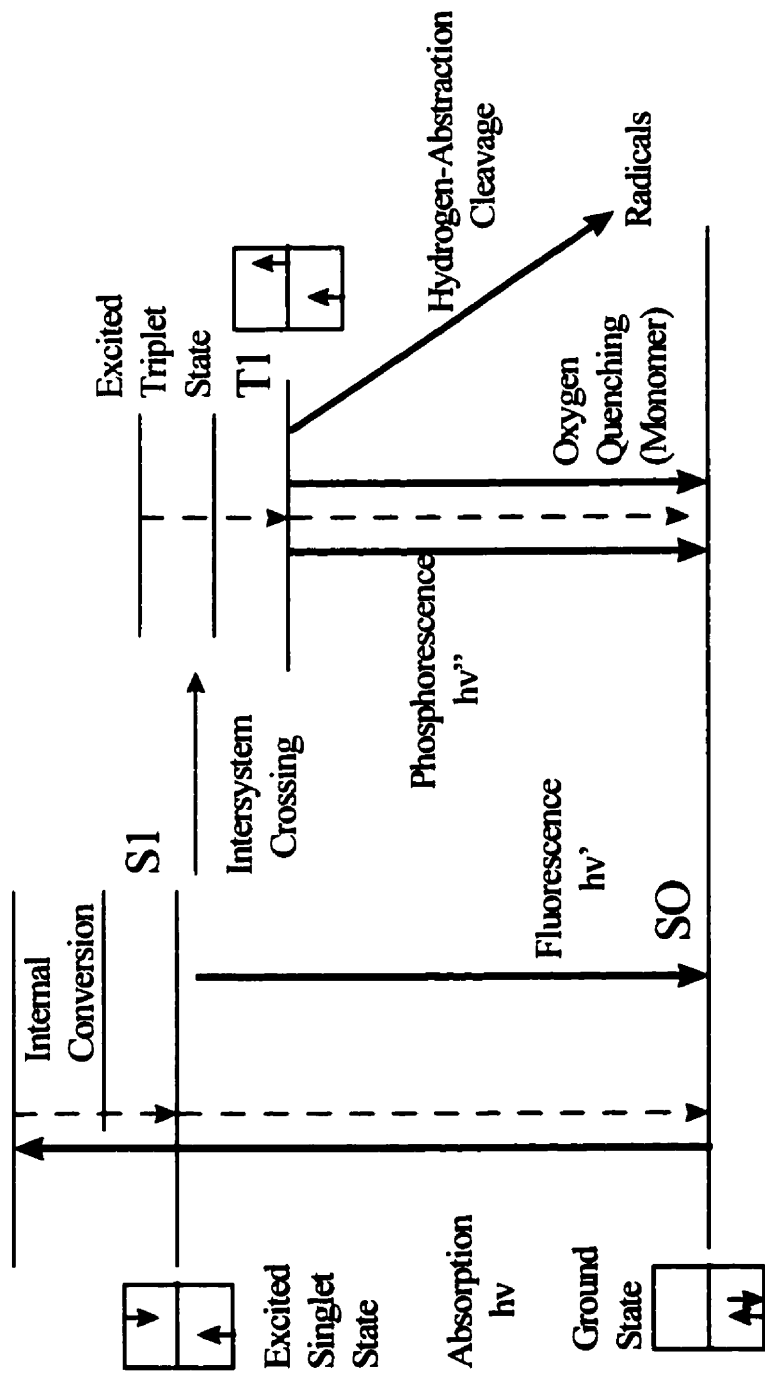
Cp @ 38 °C = 12.6 cp

Soluble in: methanol, ethanol, benzene, xylene



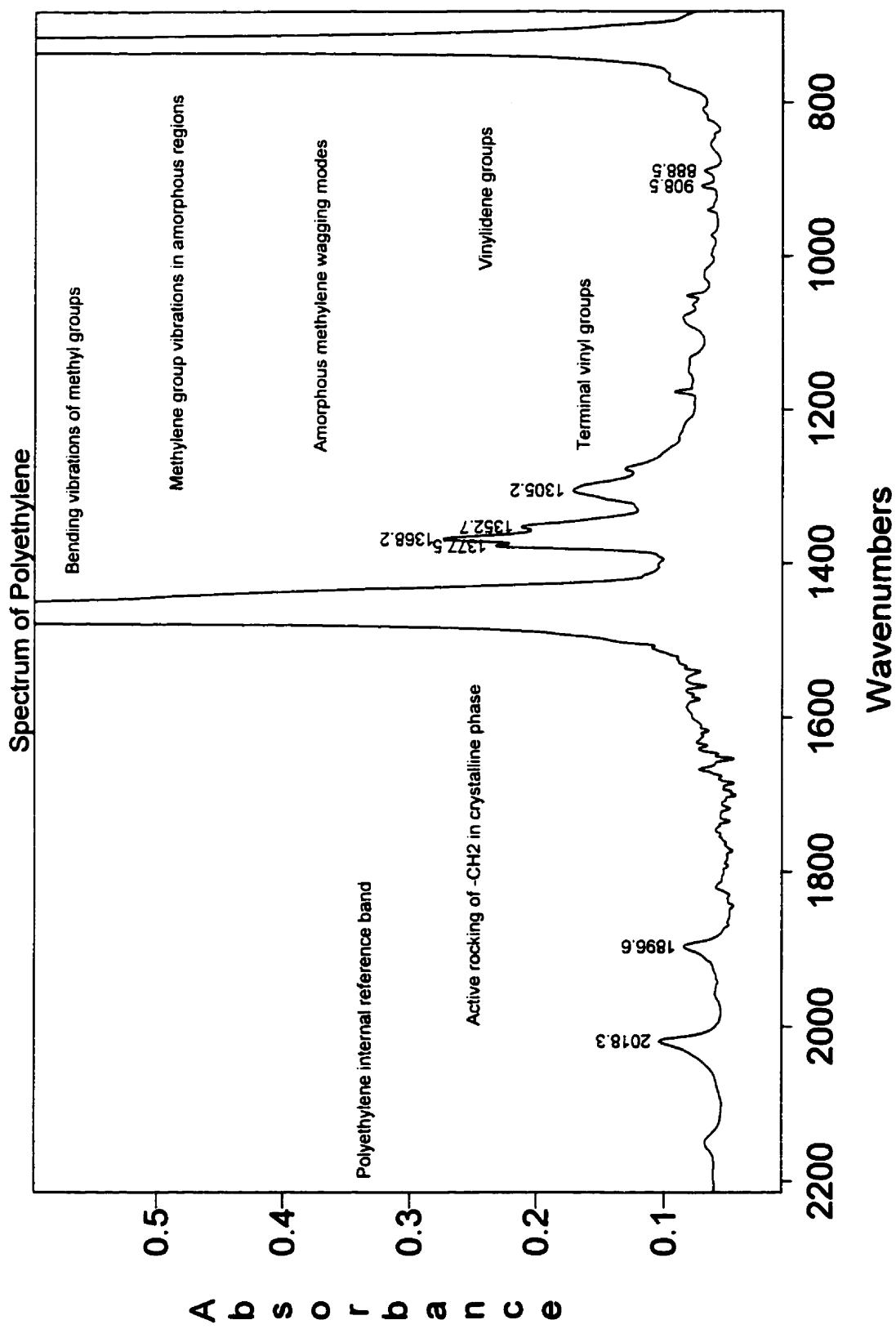
APPENDIX II: Jablonski Diagram

Jablonski Diagram



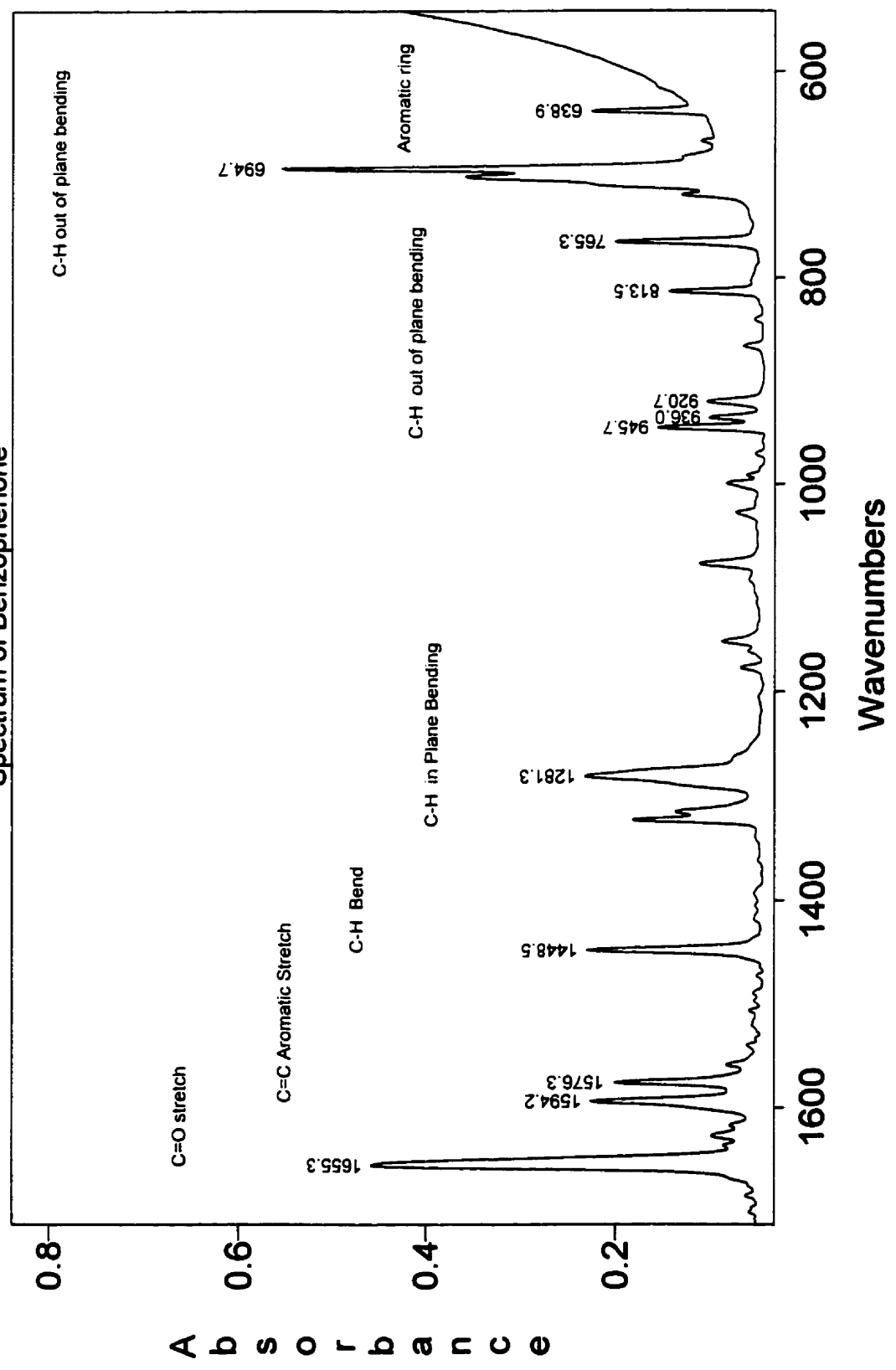
Electronic Transition Diagram

APPENDIX III: MIR Spectrum of Polyethylene, BP, and TAC



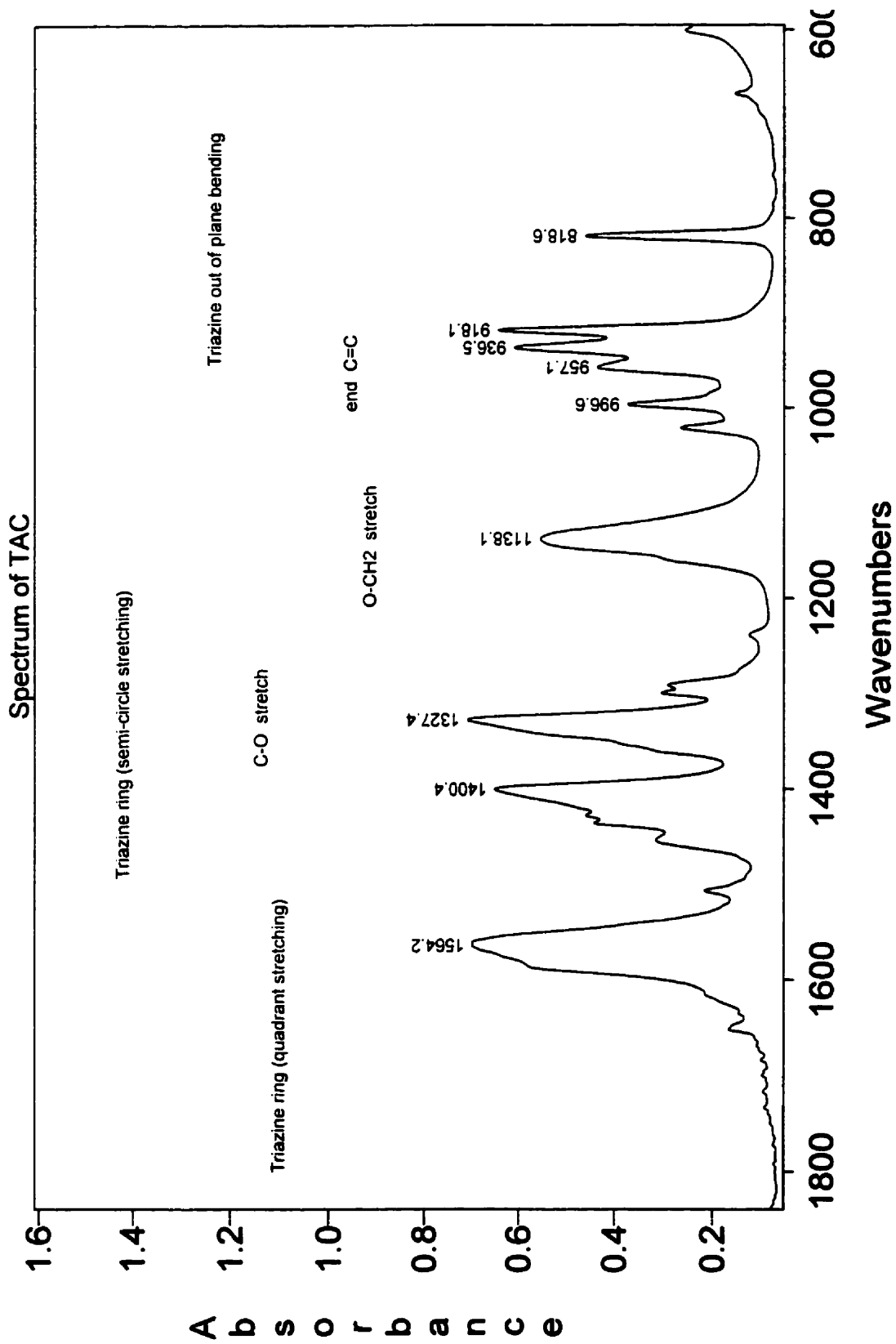
A
b
s
o
r
b
a
n
c
e

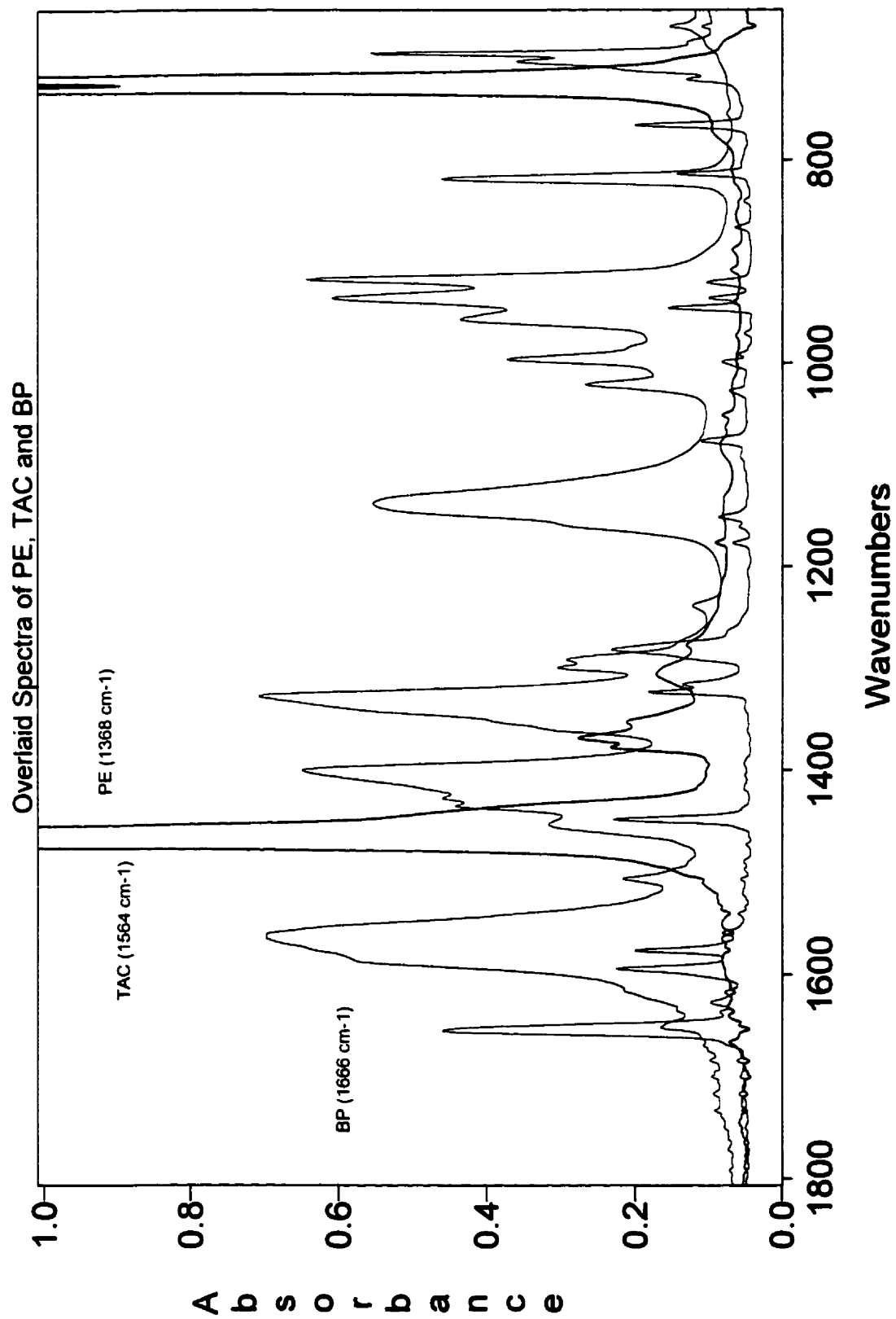
Spectrum of Benzophenone

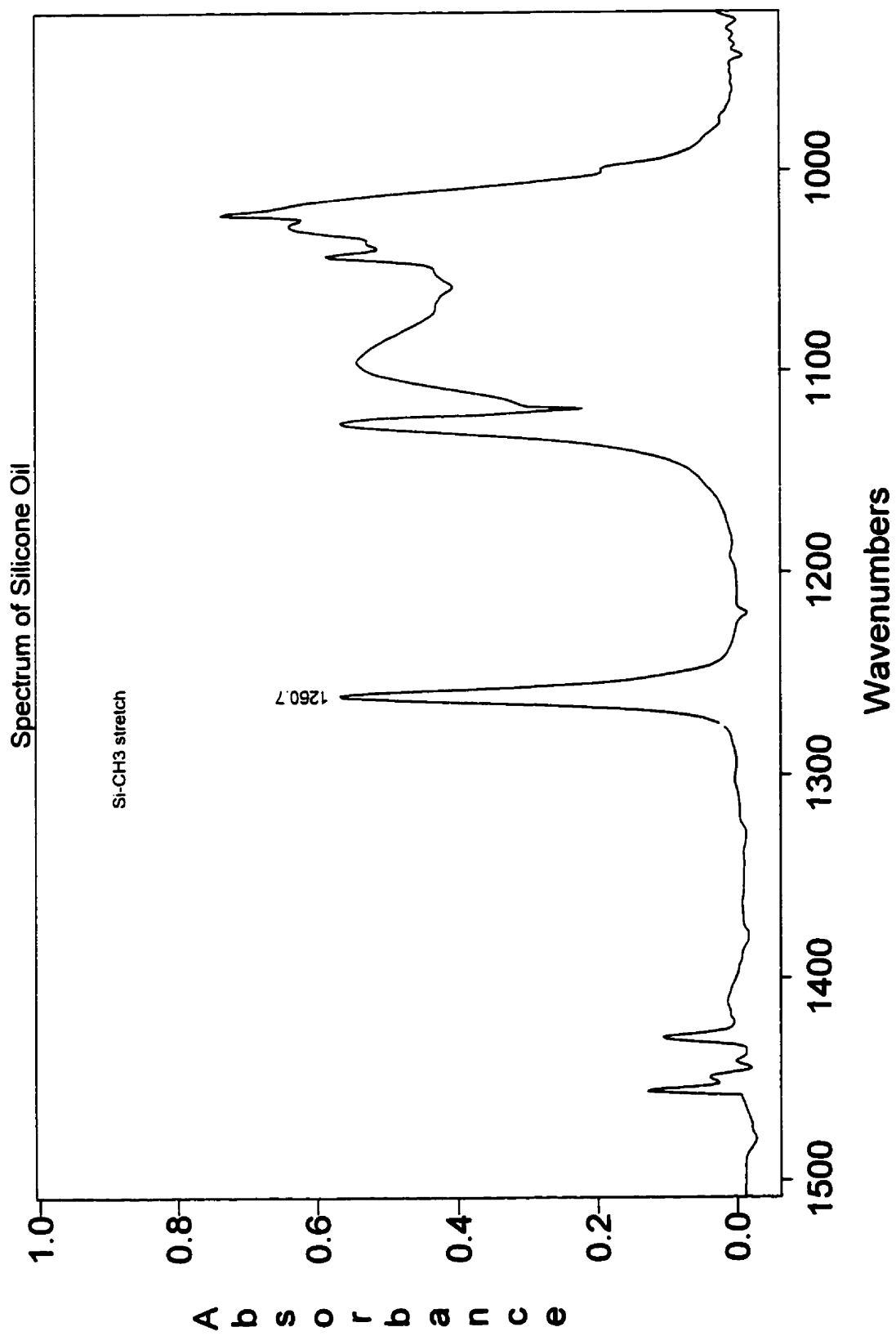


Wavenumbers

Absorbance







APPENDIX IV: Calibration Data

Calibration of BP and TAC

BP and TAC were dissolved in equal weight ratio into xylene

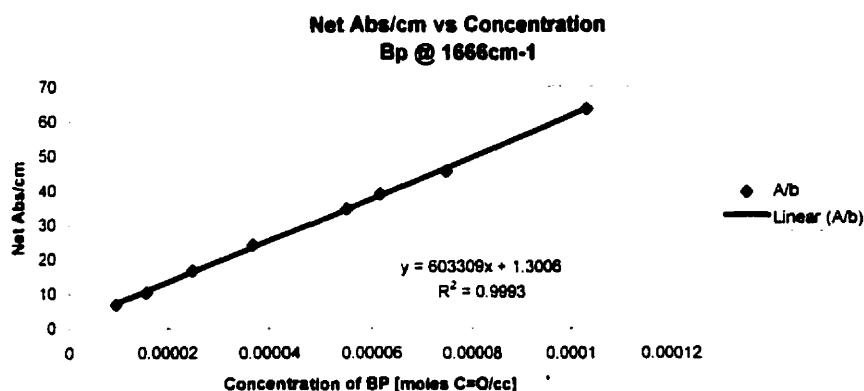
Benzophenone (C=O @1666 cm⁻¹)

Microflow cell spacer b=0.01 cm

Density of Xylene=0.866 [g/cc]

wt% BP in Xylene	[g/cc]	moles C=O/cc	Net Abs.	A/b	moles C=O/cc	A/b
0.204	0.001767	9.69509E-06	0.068	6.8	9.69509E-06	6.8
0.331	0.002866	1.57308E-05	0.103	10.3	1.57308E-05	10.3
0.526	0.004555	2.49981E-05	0.167	16.7	2.49981E-05	16.7
0.775	0.006712	3.68319E-05	0.242	24.2	3.68319E-05	24.2
1.158	0.010028	5.50339E-05	0.347	34.7	5.50339E-05	34.7
1.296	0.011223	6.15924E-05	0.389	38.9	6.15924E-05	38.9
1.572	0.013614	7.47093E-05	0.456	45.6	7.47093E-05	45.6
2.17	0.018792	0.000103129	0.635	63.5	0.000103129	63.5

BP(C=O @1666 cm⁻¹) Molar Absorptivity a = 603309 [cc /mole C=O]



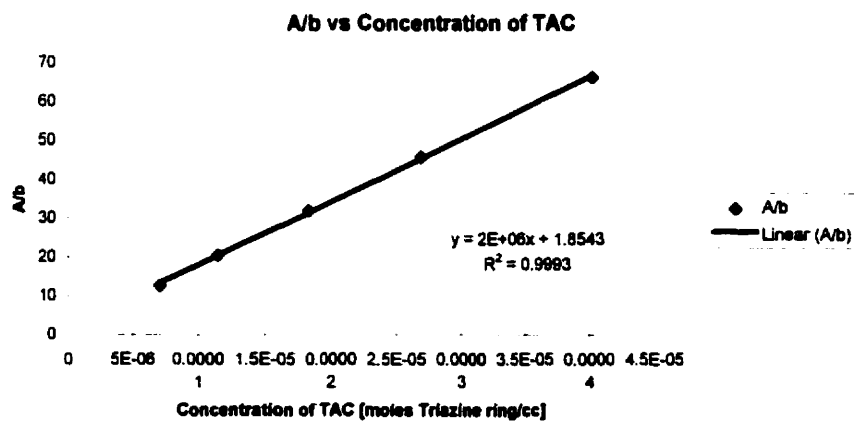
TAC (Triazine ring @ 1565 cm⁻¹)

Microflow cell spacer b=0.01 cm

Density of Xylene=0.866 [g/cc]

wt% BP in Xylene	[g/cc]	moles T.ring/cc	Net Abs.	A/b	moles T.ring/cc	A/b
0.204	0.001767	7.08725E-06	0.126	12.6	7.08725E-06	12.6
0.331	0.002866	1.14994E-05	0.205	20.5	1.14994E-05	20.5
0.526	0.004555	1.8274E-05	0.319	31.9	1.8274E-05	31.9
0.775	0.006712	2.69246E-05	0.457	45.7	2.69246E-05	45.7
1.158	0.010028	4.02306E-05	0.662	66.2	4.02306E-05	66.2

TAC (Triazine ring @1565 cm⁻¹) Molar Absorptivity a = 1611564 [cc /mole Triazine Ring]



Calibration of PB

BP and TAC were dissolved in equal weight ratio into xylene

Microflow cell spacer b=0.01 cm

Density of Xylene=0.866 [g/cc]

wt% BP in Xylene	[g/cc]	moles C=O/cc	Net Abs.	A/b	moles C=O/cc	A/b
0.204	0.001767	9.69509E-06	0.068	6.8	9.69509E-06	6.8
0.331	0.002866	1.57308E-05	0.103	10.3	1.57308E-05	10.3
0.526	0.004555	2.49981E-05	0.167	16.7	2.49981E-05	16.7
0.775	0.006712	3.68319E-05	0.242	24.2	3.68319E-05	24.2
1.158	0.010028	5.50339E-05	0.347	34.7	5.50339E-05	34.7
1.296	0.011223	6.15924E-05	0.389	38.9	6.15924E-05	38.9
1.572	0.013614	7.47093E-05	0.456	45.6	7.47093E-05	45.6
2.17	0.018792	0.000103129	0.635	63.5	0.000103129	63.5

SUMMARY OUTPUT

Regression Statistics	
Multiple R	0.99966278
R Square	0.99932587
Adjusted R Square	0.99921328
Standard Error	0.54094915
Observations	8

ANOVA					
	df	SS	MS	F	Significance F
Regression	1	2601.952994	2601.952994	8891.736	9.58462E-11
Residual	6	1.75575918	0.292625986		
Total	7	2603.70875			

	Coefficients	Standard Error	t Stat	P-value	Lower 95%	Upper 95%	Lower 95.0%	Upper 95.0%
Intercept	1.30055233	0.360244137	3.610197072	0.011228	0.419066036	2.182039	0.419066036	2.18203862
X Variable 1	603309.35	6398.037451	94.2960018	9.58E-11	587653.9047	618964.8	587653.9047	618964.7849

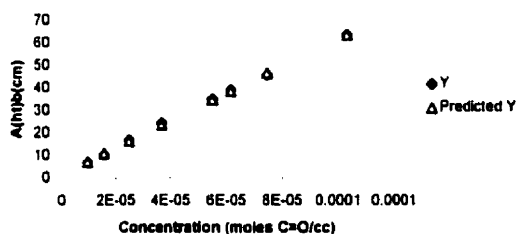
RESIDUAL OUTPUT

Observation	Predicted Y	Residuals	Standard Residuals
1	7.14969309	-0.34969309	-0.646443548
2	10.7910699	-0.491069937	-0.907793152
3	16.3821604	0.317839629	0.587559158
4	23.5215528	0.878447228	1.254179296
5	34.5030278	0.19697217	0.364123261
6	38.4597995	0.440200478	0.813755739
7	46.3733429	-0.773342906	-1.429603691
8	63.5193536	-0.019353572	-0.035777062

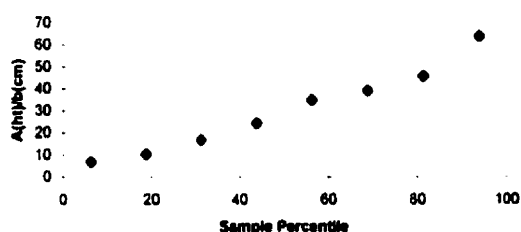
PROBABILITY OUTPUT

Percentile	Y
6.25	6.8
18.75	10.3
31.25	16.7
43.75	24.2
56.25	34.7
68.75	38.9
81.25	45.6
93.75	63.5

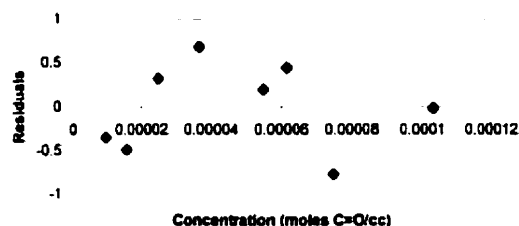
Concentration Line Fit Plot



Normal Probability Plot



Concentration Residual Plot



a = 603 309 [cc/mol C=O]

Calibration of TAC

BP and TAC were dissolved in equal weight ratio into xylene

Microflow cell spacer b=0.01 cm

Density of Xylene=0.866 [g/cc]

wt% BP in Xylene	[g/cc]	moles T.ring/cc	Net Abs.	A/b	moles T.ring/cc	A/b
0.204	0.001767	7.08725E-06	0.126	12.6	7.08725E-06	12.6
0.331	0.002866	1.14994E-05	0.205	20.5	1.14994E-05	20.5
0.526	0.004555	1.8274E-05	0.319	31.9	1.8274E-05	31.9
0.775	0.006712	2.69246E-05	0.457	45.7	2.69246E-05	45.7
1.158	0.010028	4.02306E-05	0.662	66.2	4.02306E-05	66.2

SUMMARY OUTPUT

Regression Statistics	
Multiple R	0.99964875
R Square	0.99929762
Adjusted R Square	0.99906349
Standard Error	0.65076647
Observations	5

ANOVA					
	df	SS	MS	F	Significance F
Regression	1	1807.557509	1807.557509	4288.171	7.90209E-06
Residual	3	1.27049098	0.423496993		
Total	4	1808.828			

	Coefficients	Standard Error	t Stat	P-value	Lower 95%	Upper 95%	Lower 95.0%	Upper 95.0%
Intercept	1.85433283	0.589946706	3.143220923	0.051535	-0.023142646	3.7318083	-0.02314265	3.731808304
X Variable 1	1611564.75	24667.59804	65.33123924	7.9E-06	1533061.369	1890088.1	1533061.369	1890068.129

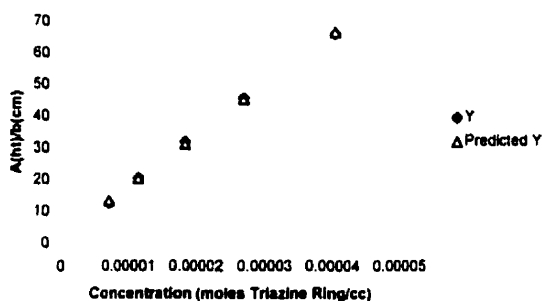
RESIDUAL OUTPUT

Observation	Predicted Y	Residuals	Standard Residuals
1	13.2759028	-0.675902807	-1.038625747
2	20.38639	0.113610001	0.174578757
3	31.3040672	0.595932816	0.915739896
4	45.2451011	0.454898872	0.699020149
5	66.6885389	-0.488538881	-0.750713054

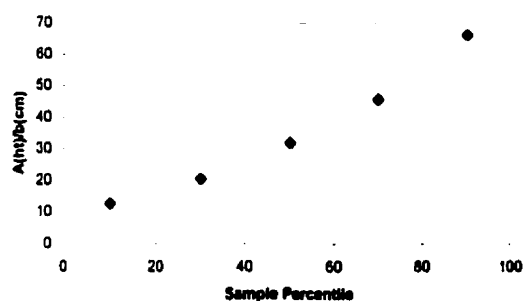
PROBABILITY OUTPUT

Percentile	Y
10	12.6
30	20.5
50	31.9
70	45.7
90	66.2

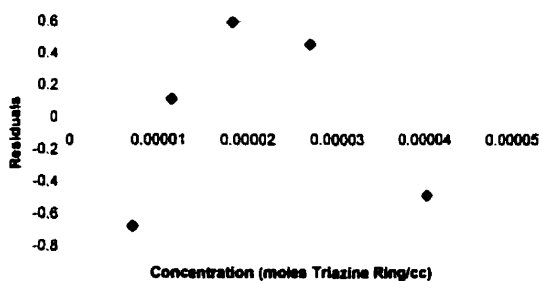
Concentration Line Fit Plot



Normal Probability Plot



Concentration Residual Plot



a = 1 611 565 [cc/mole Triazine Ring]

Calibration of BP (C=O @1666 cm-1)

BP, TAC, and Silicone oil were dissolved in equal weight ratio into xylene

[g/ml]	[moles C=O/ml]	Net Abs./cm
0.00304	1.66831E-05	10.41
0.00608	3.33663E-05	20.84
0.01255	6.88728E-05	42.15

SUMMARY OUTPUT

Regression Statistics	
Multiple R	0.999950812
R Square	0.999901627
Adjusted R Square	0.999803255
Standard Error	0.226919554
Observations	3

ANOVA

	df	SS	MS	F	Significance F
Regression	1	523.3913742	523.3913742	10164.42	0.00631429
Residual	1	0.051492484	0.051492484		
Total	2	523.4428667			

	Coefficients	Standard Error	t Stat	P-value	Lower 95%	Upper 95%	Lower 95.0%	Upper 95.0%
Intercept	0.408198048	0.272229412	1.49946343	0.374439	-3.050789776	3.867186	-3.05078978	3.867185872
X Variable 1	606912.8959	6019.840816	100.8187616	0.006314	530423.8937	683401.9	530423.8937	683401.8981

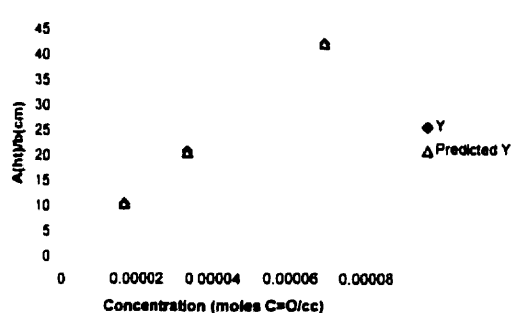
RESIDUAL OUTPUT

Observation	Predicted Y	Residuals	Standard Residuals
1	10.53340496	-0.123404961	-0.543826913
2	20.65861187	0.181388126	0.799349914
3	42.20798317	-0.057983165	-0.255523001

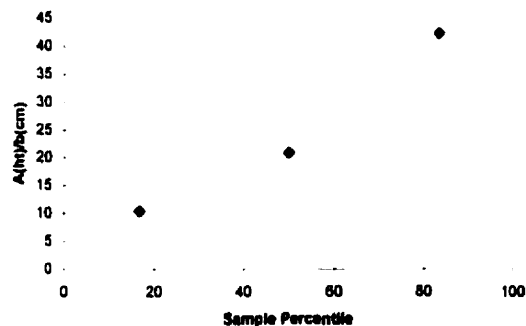
PROBABILITY OUTPUT

Percentile	Y
16.66666667	10.41
50	20.84
83.33333333	42.15

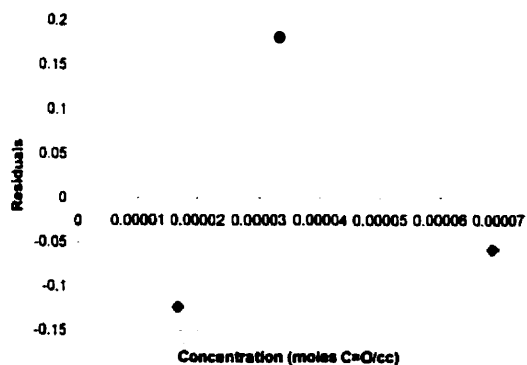
Concentration Line Fit Plot



Normal Probability Plot



Concentration Residual Plot



$a = 606\,913$ [cc/mole C=O]

Calibration of TAC (Triazine Ring @1565 cm-1)

BP, TAC, and Silicone oil were dissolved in equal weight ratio into xylene

[g/ml]	[moles Tr.Ring/ml]	Net Abs./cm
0.00304	1.21956E-05	19.49
0.00608	2.43912E-05	39.1
0.01255	5.0347E-05	80.04

SUMMARY OUTPUT

Regression Statistics	
Multiple R	0.99998917
R Square	0.99997834
Adjusted R Square	0.99995668
Standard Error	0.20333411
Observations	3

ANOVA

	df	SS	MS	F	Significance F
Regression	1	1908.938055	1908.938055	46171.22	0.002982725
Residual	1	0.04134476	0.04134476		
Total	2	1908.9794			

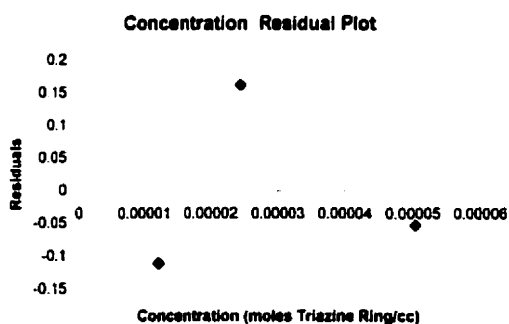
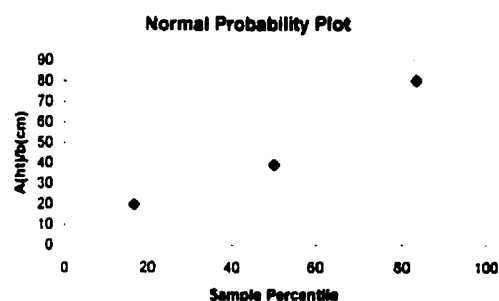
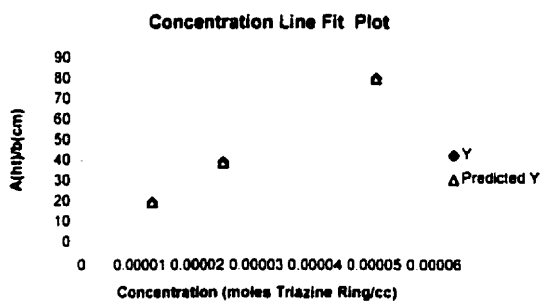
	Coefficients	Standard Error	t Stat	P-value	Lower 95%	Upper 95%	Lower 95.0%	Upper 95.0%
Intercept	0.26369222	0.243934574	1.080995692	0.475234	-2.835777141	3.3631616	-2.83577714	3.363161589
X Variable 1	1585561.07	7378.996317	214.8748967	0.002963	1491802.435	1679319.7	1491802.435	1679319.708

RESIDUAL OUTPUT

Observation	Predicted Y	Residuals	Standard Residuals
1	19.6005786	-0.110578561	-0.543826913
2	38.9374649	0.162535103	0.799349914
3	80.0919565	-0.051956542	-0.255523001

PROBABILITY OUTPUT

Percentile	Y
16.66666667	19.49
50	39.1
83.33333333	80.04



a = 1 585 561 [cc/mole Triazine Ring]

Variation of molar absorptivity a :

BP (C=O @1666 cm⁻¹): 0.59%

TAC (Triazine Ring @1565 cm⁻¹): 1.6%

Calibration of Silicone Oil (Si-CH₃ @1260.7 cm⁻¹)

BP, TAC, and Silicone oil were dissolved in equal weight ratio into xylene

[g/ml]	[moles Si-CH ₃ /cc]	Net Abs./cm
0.00304	2.23283E-05	7.69
0.00608	4.46566E-05	15.49
0.01255	9.21777E-05	31.92

SUMMARY OUTPUT

Regression Statistics	
Multiple R	0.9999969
R Square	0.9999938
Adjusted R Square	0.9999876
Standard Error	0.043607
Observations	3

ANOVA

	df	SS	MS	F	Significance F
Regression	1	305.9573651	305.9573651	160897.1	0.001587103
Residual	1	0.001901572	0.001901572		
Total	2	305.9592667			

	Coefficients	Standard Error	t Stat	P-value	Lower 95%	Upper 95%	Lower 95.0%	Upper 95.0%
Intercept	-0.0277134	0.05231419	-0.5297491	0.689863	-0.692425357	0.63699857	-0.69242536	0.63699857
X Variable 1	346709.02	864.3528564	401.1197751	0.001587	335726.4261	357691.621	335726.426	357691.621

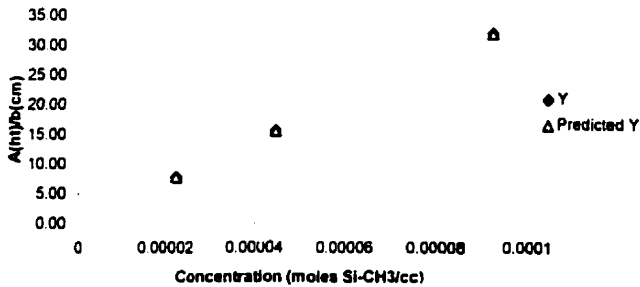
RESIDUAL OUTPUT

Observation	Predicted Y	Residuals	Standard Residuals
1	7.7137147	-0.02371467	-0.543826913
2	15.455143	0.034857266	0.799349914
3	31.931143	-0.011142596	-0.255523001

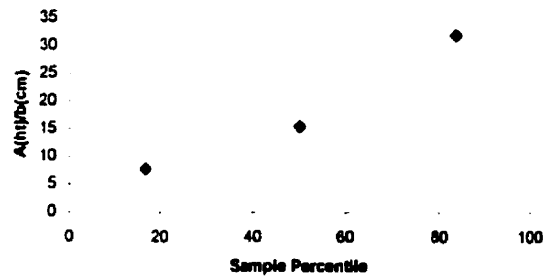
PROBABILITY OUTPUT

Percentile	Y
16.66666667	7.69
50	15.49
83.33333333	31.92

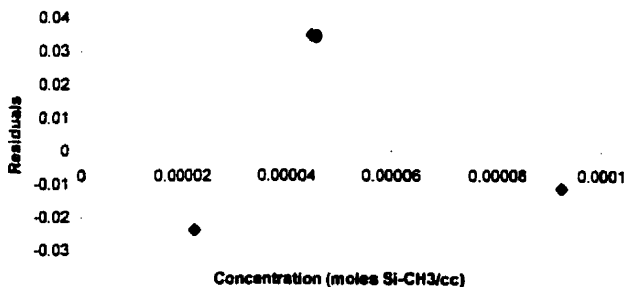
Concentration Line Fit Plot



Normal Probability Plot



Concentration Residual Plot



a = 346 709 [cc/mole Si-CH₃]

APPENDIX V: Derivation of Equations and Sample Calculations

APPENDIX V : Derivation of Equations:

I Concentration of BP in PE

$$A=abc$$

$a=A/(bc)$ =Net absorbance (unitless)/[concentration (moles C=O/cm³)*path length (cm)]
 = cm² / (moles C=O)
 = slope of calibration curve dissolving 0.204, 0.331, 0.526, 0.775, 1.158, 1.296, 1.572, and 2.17 wt% in xylene

$$\text{Concentration (c)} = A(\text{ht}) / ab = A / [a (\text{moles C=O/cm}^3) * b (\text{cm})] = \text{moles C=O/cm}^3$$

$$c (\text{g BP/cm}^3) = c (\text{moles BP/ cm}^3) * \text{Mw BP (g BP/mole BP)}$$

$$= c (\text{moles C=O/cm}^3) * 1 \text{ mole BP/ 1 mole C=O}$$

wt% BP in PE = g BP/g PE * 100 [%] = [g BP/cm³] / [ρ_{PE} (g PE/cm³)] * 100
 After substitution of : a=603309
 Mw=182.22
 ρ_{PE} = 0.959

we received:

$$\text{wt\% BP in PE} = 0.0315 * A/b$$

II Concentration of TAC in PE

$$A=abc$$

$a=A/(bc)$ = Net absorbance (unitless)/[concentration (moles Triazine ring/cm³) * path length (cm)]
 = cm² / (moles Triazine ring)
 = slope of calibration curve dissolving 0.204, 0.331, 0.526, 0.775, and 1.158 wt% in xylene.

$$\text{Concentration (c)} = A(\text{ht}) / ab = A / [a (\text{moles Triazine ring/cm}^3) * b (\text{cm})] = \text{moles Triazine ring/cm}^3$$

$$c (\text{g TAC/cm}^3) = c (\text{moles TAC/ cm}^3) * \text{Mw TAC (g TAC/mole TAC)}$$

$$= c (\text{moles Triazine ring/cm}^3) * 1 \text{ mole TAC/ 1 mole Triazine ring}$$

wt% TAC in PE = g TAC/g PE * 100 [%] = [g TAC/cm³] / [ρ_{PE} (g PE/cm³)] * 100
 After substitution of : a=1611564
 Mw=249.27
 ρ_{PE} = 0.959

we received:

$$\text{wt\% TAC in PE} = 0.0161 * A/b$$

III. Concentration of Silicone Oil in PE

$$A = abc$$

$$a = A/(bc) = \text{Net absorbance (unitless)} / [\text{concentr. (moles Si-CH}_3/\text{cm}^3) * \text{path length (cm)}]$$

$$= \text{cm}^2 / (\text{moles Si-CH}_3)$$

= slope of calibration curve dissolving 0.304, 0.608, and 1.255 g/100 ml in xylene.

$$\text{Concentration (c)} = A(\text{ht}) / ab = A / [a (\text{moles Si-CH}_3/\text{cm}^3) * b (\text{cm})] =$$

$$= \text{moles Si-CH}_3/\text{cm}^3$$

$c (\text{g TAC}/\text{cm}^{-3}) = c (\text{moles Silicone Oil}/\text{cm}^{-3}) * \text{Mw Silicone Oil (g Silicone Oil/mole Silicone Oil)}$

$$= c (\text{moles Si-CH}_3/\text{cm}^{-3}) * 1 \text{ mole Silicone Oil} / 1 \text{ mole Si-CH}_3$$

$\text{wt}\% \text{ Silicone Oil in PE} = \text{g Silicone Oil/g PE} * 100 [\%] = [\text{g Silicone Oil}/\text{cm}^{-3}] / [\rho_{\text{PE}} (\text{g PE}/\text{cm}^{-3})] * 100$

After substitution of : $a = 346\ 709$


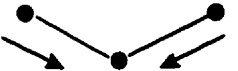
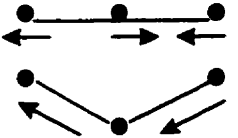

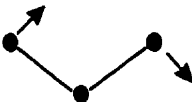

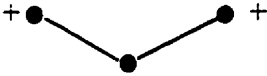

$$\text{Mw} = 136.15$$

$$\rho_{\text{PE}} = 0.959$$

we received:

$$\text{wt}\% \text{ Silicone Oil in PE} = 0.0409 * A/b$$

APPENDIX VI: List of Selected Vibrational Modes

Type of vibration	Designation
Stretching vibration	
	Symmetrical stretching vibration
	
	Asymmetrical stretching vibration
Bending (deformation) vibrations	
	Scissoring vibration in-plane
	Rocking vibration in plane
	Wagging vibration out-of-plane
	
	Twisting (torsion) vibration

APPENDIX VII : Analysis of Variance for 2^3 Factorial Design

APPENDIX VII : Analysis of Variance for 2³ Factorial Design

1. Analysis of Variance Table for Loss of Benzophenone

Source of variation (Factor)	Sum of squares (SS)	Degrees of freedom (DF)	Mean square MS (SS/DF)	Mean-Square ratio MSR (MS/MS _{residual})	F(0.05,1,4)
Residence time (A)	39.87245	1	39.87245	1.247149	7.71
Barrel temperature (B)	8.9042	1	8.9042	0.27851	7.71
Die temperature (C)	30.96845	1	30.96845	0.968646	7.71
AB interaction	1.56645	1			
AC interaction	0.2592	1			
BC interaction	50.90405	1			
ABC interaction	75.1538	1			
Residual (error) term	127.8835	4	31.97088		

2. Analysis of Variance Table for Loss of TAC

Source of variation (Factor)	Sum of squares (SS)	Degrees of freedom (DF)	Mean square MS (SS/DF)	Mean-Square ratio MSR (MS/MS _{residual})	F(0.05,1,4)
Residence time (A)	10.14751	1	10.14751	3.715728	7.71
Barrel temperature (B)	2.050313	1	2.050313	0.750766	7.71
Die temperature (C)	1.336613	1	1.336613	0.489429	7.71
AB interaction	3.685613	1			
AC interaction	1.044013	1			
BC interaction	4.455113	1			
ABC interaction	1.739113	1			
Residual (error) term	10.92385	4	2.730963		